TM-75749

NASA TECHNICAL MEMORANDUM

NASA TM-75749

# A FINITE ELEMENT METHOD FOR THE COMPUTATION OF TRANSONIC FLOW PAST AIR FOILS

A. Eberle

Translation of "Eine Methode finiter Elemente zur Berechnung der transsonischen Potential-Stroemung um Profile," Messerschmidt-Boelkow G.m.b.H. Munich (West Germany), Report No. MBB-UFE-1352-0, 23 Sept. 1977, pp 1-63



NATIONAL AERONAUTICS AND SPACE ADMINISTRATION
WASHINGTON, D.C. FEBRUARY 1980

Contents

Symbols

| | |
|---|---|
| $A$ | work |
| $a$ | polynomial coefficient |
| $B$ | flow regime |
| $b$ | polynomial coefficient |
| $C$ | airfoil contour |
| $c$ | polynomial coefficient |
| $D$ | Jacobi determinant, dipole, thickness |
| $d$ | polynomial coefficient |
| $e$ | influence function, polynomial coefficient |
| $\varepsilon$ | circle region, viscosity parameter |
| $\eta$ | image coordinates |
| $f$ | function, polynomial coefficient |
| $\phi$ | potential |
| $\overline{\phi}$ | approximated potential |
| $\varphi$ | disturbance potential |
| $G$ | form function |
| $\Gamma$ | circulation |
| $\gamma$ | circle central angle |
| $H$ | auxiliary point, hyperbolic point |
| $I$ | element energy |
| $K$ | corridor, power |
| $\varkappa$ | adiabatic exponent |
| $L$ | contour slot |
| $M$ | Mach number |
| $m$ | singularity centroid |

| | |
|---|---|
| $n$ | boundary normals |
| $o$ | "above" |
| $p$ | pressure |
| $P$ | control point |
| $q$ | velocity |
| $\bar{q}$ | normalized velocity |
| $R$ | residuum |
| $r$ | radius |
| $\varrho$ | density |
| $s$ | boundary abscissa, stream line path |
| $\vartheta$ | angle, unit eddy potential |
| $u$ | velocity components, "below" |
| $w$ | velocity components |
| $x$ | abscissa |
| $\xi$ | image abscissa |
| $z$ | ordinate |
| $\zeta$ | Prandtl ordinate |
| $\circ$ | "zero", "ram" |
| $\bullet$ | "sound" |

List of figures

## 1. Introduction

/1

Processes developed to date for calculating the transonic potential flow around airfoils and simple three-dimensional configurations depend for their evaluation on difference schemes which all require a rectangular coordinate system.

For airfoils it is also important to set up a conformal premapping to a circle where radii and concentric circles form a natural rectangular coordinate system. However, for the three-dimensional case such a process is hardly possible and besides, because of the after-differentiations would lead to quite complicated mathematical expressions.

The purpose of the present effort was to develop a method which operates exclusively directly in a physical plane so that nothing would prevent an extension to three dimensions.

With certain limitations finite-element methods need not depend on orthogonal networks. However, they have a number of grave disadvantages:

- The solution depends on the element type. When the network is refined, methods with different elements converge to different results, and only in special cases do they lead to an exact solution.

- The stream velocity is always underestimated. This is especially important for the transonic region where the magnitudes and the positions of compression shocks depend to a great degree on the velocity field.

- The proofs for convergence found in the literature are wrong.

/2

- Although structural mechanics offer hundreds of element types, only one even approximately satisfies the accuracy requirements of progressive numerical aerodynamics.

The last two items, in particular, create great difficulties in the development of the methods since one is forced to use computer-intensive cut-and-try methods. An extensive study has shown that, in a strictly mathematical sense the simple elements converge to an exact solution only when they are distributed across the flow field in an orthogonal combination. For then such a method degenerates to a difference scheme.

As always, the best aerodynamic element is the plane panel which, a priori, includes a non-trivial solution of the potential equation. However, it has not been possible to date to carry this over to the treatment of transonic flow problems.

Thanks to a careful choice of the element and to the introduction of artificial viscosity, without which it would not at all be possible to achieve iterative convergence, the subject effort can at least be considered an engineering breakthrough of the finite-element method for transonic flow problems; however, the results shown in the literature to date must be considered harmless, such as subsonic flow around circles, Joukowski airfoils and simple NACA airfoils whose field, in addition was often calculated in an approximately circular image plane, where the actual problems of the finite-element technique do not even come into play.

## 2. Basic Equations

/3

We shall base the mathematical formulation of our problem on the stationary, rotation-free, and isoenergetic flow of a completely ideal gas.

There will be no sources if the continuity equation

$$(\varrho u)_x + (\varrho w)_z = 0 \qquad (1)$$

and there will be rotational freedom if

$$u_z = w_x \tag{2}$$

is satisfied.

The energy carried along by the fluid element is to be constant in the entire flow field:

$$q^2 = u^2 + w^2$$

$$\frac{2\varkappa}{\varkappa-1}\frac{p}{\varrho} + q^2 = \frac{2\varkappa}{\varkappa-1}\frac{p_0}{\varrho_0} \tag{3}$$

Since we assumed irrotational flow, the changes of state are considered to be isentropic:

$$p = p_0 \left(\frac{\varrho}{\varrho_0}\right)^{\varkappa} \tag{4}$$

For completeness sake we shall introduce the Mach number so that we can differentiate as to supersonic or subsonic flow:

$$\varkappa\frac{p}{\varrho} = \frac{a^2}{M^2}$$

In (3):

$$q^2 = \varkappa\frac{p_0 M^2}{\varrho_0\left(1 + \frac{\varkappa-1}{2}M^2\right)} \tag{5}$$

## 3. Normalization

Equations (3), (4), and (5) contain an unknown constant which can be easily removed if we define a dimensionless velocity $\bar{q}$ according to

$$q^2 = \varkappa\frac{p_0}{\varrho_0}\bar{q}^2$$

Then from equation (3) we get:

$$\frac{\varrho_0}{p_0}\frac{p}{\varrho} + \frac{\varkappa-1}{2}\bar{q}^2 = 1 \tag{6}$$

from (5) we get:

$$q^2 = \frac{M^2}{1 + \frac{\kappa-1}{2} M^2} \tag{7}$$

substituting (4) into (6) gives:

$$\varrho = \varrho_0 \left(1 - \frac{\kappa-1}{2} q^2\right)^{\frac{1}{\kappa-1}} \tag{8}$$

From (7) we can obtain the sonic velocity (M = 1) to be:

$$q^2 = \frac{2}{\kappa+1}$$

If we now understand that the uncancelled values represent the corresponding normalized values, then equations (1) and (2) remain unchanged.

## 4. The Far-Field Solution /5

### 4.1 Prandtl Transformation

Independent of any further procedure the flow far downstream of the given airfoil can be estimated if equation (1) is made linear. Here we differentiate (1) to:

$$u\varrho_x + \varrho u_x + w\varrho_z + \varrho w_z = 0.$$

The parallel onflow is disturbed only weakly so that in the following the vertical velocity component w can be neglected:

$$u\varrho_x + \varrho u_x + \varrho w_z = 0 \tag{9}$$

can be determined by after-differentiation from (8)

$$u\varrho_x = q\varrho_{q^2} q^2{}_x = -\frac{q^2 \varrho\, q_x}{1 - \frac{\kappa-1}{2} q^2}$$

This can be written more simply if we replace $q^2$ by equation (7)

$$u\varrho_x = q\varrho_x = -M^2 \varrho\, q_x \tag{10}$$

At infinity the Mach number will deviate only little from the incident Mach number so that with (10) equation (9) simplifies to

$$(1 - M_\infty^2)\, u_x + w_z = 0 \quad . \tag{11}$$

Equation (2) permits the introduction of a potential according to

$$u = \phi_x \tag{12}$$
$$w = \phi_z \tag{13}$$

so that (11) becomes

$$(1 - M_\infty^2)\, \phi_{xx} + \phi_{zz} = 0$$

From that we can form the Laplace equation is transformed with

$$\zeta = \sqrt{1 - M_\infty^2}\; z \tag{14}$$

This then produces:

$$\phi_{xx} + \phi_{\zeta\zeta} = 0 \tag{15}$$

## 4.2 Integral potential representation

If we substitute the expression

$$\phi = u_\infty x + w_\infty z + \varphi \tag{16}$$

into (15), then obviously the following equation must be solved:

$$\varphi_{xx} + \varphi_{\zeta\zeta} = 0 \tag{17}$$

To do this we use Green's theorem

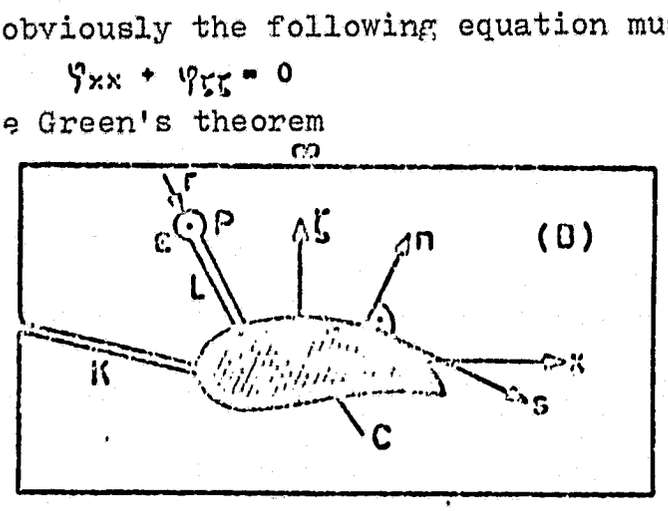


We multiply (17) by an influence function e yet to be determined and integrate over (B)

$$\iint_{(B)} e(\varphi_{xx}+\varphi_{\zeta\zeta})\,dx\,d\zeta = \oint_{CK\infty LC} e\varphi_n\,ds - \iint_{(B)-KLC} (e_x\varphi_x + e_\zeta\varphi_\zeta)\,dx\,d\zeta = 0 \tag{18}$$

Exchanging e with $\varphi$, we obtain analogously

$$\iint_{(B)-KL\mathcal{E}} \varphi(e_{xx}+e_{\zeta\zeta})\,dx\,d\zeta = \oint_{CK\mathcal{E}L} \varphi e_n\,ds - \iint_{(B)-KL\mathcal{E}} (e_x\varphi_x + e_\zeta\varphi_\zeta)\,dx\,d\zeta$$

The surface integral on the right is replaced by (18): /7

$$\oint_{CK\mathcal{E}L} \varphi e_n\,ds - \oint_{CK\mathcal{E}L} e\varphi_n\,ds = \iint_{(B)-KL\mathcal{E}} \varphi(e_{xx} + e_{\zeta\zeta})\,dx\,d\zeta$$

The contour pieces L and K make no contribution since the derivatives cancel each other over the forward and return path.

Similarly the contribution of the outer border disappears at infinity since there is pure parallel flow so that according to equation (16) the disturbance potential must disappear identically. Thus the following remains

$$\oint_{\mathcal{E}} \varphi e_n\,ds = \oint_{\mathcal{E}} e\varphi_n\,ds + \oint_{\mathcal{C}} (e\varphi_n - \varphi e_n)\,ds + \iint_{(B)-\mathcal{E}} \varphi(e_{xx}+e_{\zeta\zeta})\,dx\,d\zeta$$

The left integral can be evaluated immediately if $\mathcal{E}$ is small and if e is exclusively of function of the radius because then the integrand over the circle $\mathcal{E}$ is constant.

$$\oint_{\mathcal{E}} \varphi e_n\,ds = \int_0^{2\pi} \varphi_p\, e_r\, r\, d\varphi = \varphi_p\, e_r\, r\, 2\pi$$

If we now demand that

$$e_r\, r\, 2\pi = 1$$

then it follows that

$$e = \frac{1}{2\pi} \ln r$$

If we substitute this result into the integral equation and if we allow $\mathcal{E}$ to shrink toward 0, then we finally obtain

$$\varphi_p = \frac{1}{2\pi} \oint \left[\varphi_n \ln r - \varphi(\ln r)_n\right] ds \qquad (19)$$

where the integral must be taken over the edges of the airfoil.

## 4.3 Displacement Term

/8

We are seeking an approximation solution for the first integral of (19) for a slender airfoil. Then the following approximation becomes valid:

$$\frac{\partial}{\partial n} = \frac{\partial}{\partial \zeta}$$

$$ds = dx$$

$$\varphi_D = \frac{1}{2\pi} \oint \varphi_\zeta \ln r \, dx$$

or with (14)

$$\varphi_D = \frac{1}{2\pi\sqrt{1 - M_\infty^2}} \oint \varphi_z \ln r \, dx$$

For disappearing supersonic velocities the linearized boundary condition

$$\varphi_z = u_\infty z'$$

is valid from which, by partial integration, we get

$$\varphi_D = \frac{U_\infty}{2\pi\sqrt{1 - M_\infty^2}} \left[ z \ln r \Big|_0^\circ - \oint z \, (\ln r)_x \, dx \right]$$

For smooth closed profiles the first term drops out. From

$$r = \sqrt{(x_p - x)^2 + (\zeta_p - \zeta)^2}$$

and equation (14) we get

$$\varphi_D = \frac{U_\infty}{2\pi\sqrt{1 - M_\infty^2}} \oint z \frac{(x_p - x) \, dx}{(x_p - x)^2 + (1 - M_\infty^2)(z_p - z)^2}$$

At infinity the profile irregularities at x, z become point-shaped so that in approximation we obtain

$$\varphi_D = \frac{U_\infty}{2\pi\sqrt{1 - M_\infty^2}} \frac{(x_p - x_m)}{(x_p - x_m)^2 + (1 - M_\infty^2)(z_p - z_m)^2} \oint z \, dx \qquad (20)$$

The singularity points $x_m$, $z_m$ must be placed on the inside of the airfoil. The boundary integral becomes the airfoil surface.

## 4.4 Eddy Term



The second integral in (19) can be evaluated as follows:

$$\varphi_{\Gamma} = -\frac{1}{2\pi}\oint \gamma (\ln r)_n \, ds =$$

$$= \frac{1}{2\pi}\oint \gamma \frac{n_p}{(s_p - s)^2 + n_p^2} \, ds$$

$$= -\frac{1}{2\pi}\oint \gamma \left[\operatorname{atan}\frac{s_p - s}{n_p}\right]_s \, ds =$$

$$= -\frac{1}{2\pi}\oint \gamma \, d \operatorname{atan}\frac{s_p - s}{n_p}$$

$$= -\frac{1}{2\pi}\oint \gamma \, d\vartheta$$

where $d\vartheta$ is the angle increment viewed from control point P.

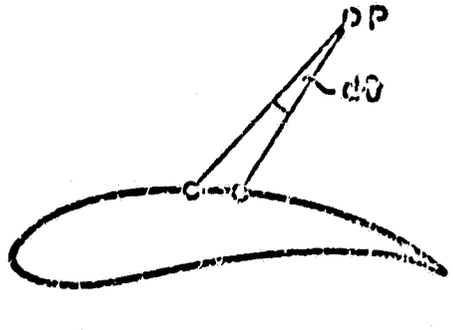


Partial integration:

$$\varphi_{\Gamma} = -\frac{1}{2\pi}\left(\gamma\vartheta\Big|_0^{\circ} - \oint \vartheta \, d\gamma\right) = \frac{1}{2\pi}\oint \vartheta \, d\gamma$$

At a great distance from the airfoil the change of angle disappears so that one can make the approximation

$$\varphi_{\Gamma} = \frac{\vartheta}{2\pi}\oint d\gamma = \frac{\vartheta}{2\pi}\Delta\gamma = \Gamma\vartheta$$

With (14)

$$\varphi_{\Gamma} = \Gamma \operatorname{atan}\frac{(z_p - z_m)\sqrt{1 - M_\infty^2}}{x_p - x_m} \qquad (21)$$

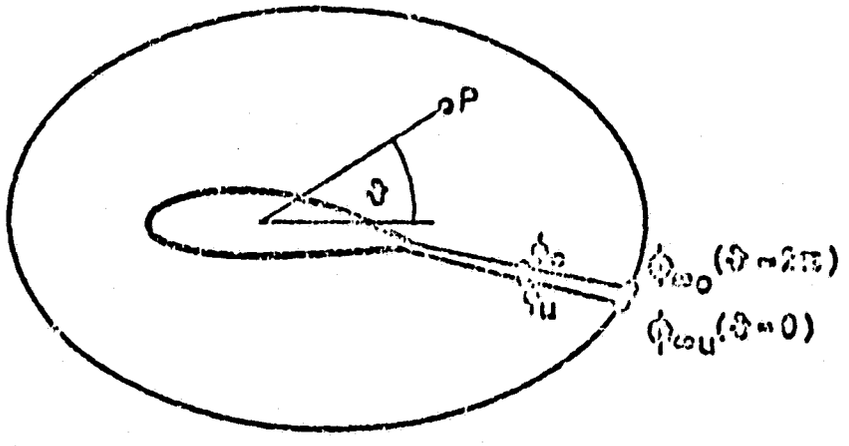


At the circulation slot the velocity is equal on both sides so that, surely, the following is true:

$$n\phi - n\omega\phi = o\phi - o\omega\phi$$

With the value for $\phi_\Gamma$, one obviously obtains

$$\phi_u - \phi_o = -\Gamma 2\pi \qquad (22)$$

The potential jump thus is constant over the entire circulation slot.

## 5. Modification of the Continuity Equation for Transonic Flow

### 5.1 Dependence on Direction

If at point P we calculate the velocity on which all gas-dynamic values depend according to our theory, then we approach the control point P from both sides as we form the boundary value of the potential-differential quotient along the stream line s.

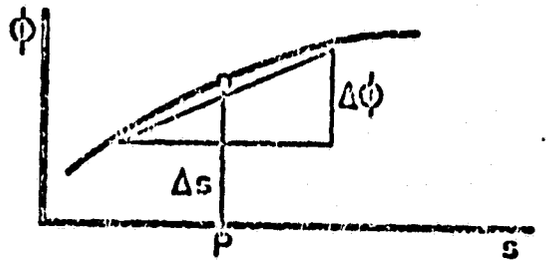


The velocity thus always depends on a potential value ahead of and behind the control point, viewed in flow direction, regardless of how close one comes to the control point.

For supersonic flow downstream of the control point signals are carried downstream at a faster rate than the expansion velocity of disturbances, flowing in the opposite direction, can carry them back to the control point.

Thus the control point can only be influenced by events occurring upstream. Obviously for this case the described Cauchy potential derivation is not correct. On the contrary it is necessary that the velocity be generated at an auxiliary point H located upstream of the control point P. Here the distance H-P can be very small.

Therefore we develop the following mathematical model: /12
For subsonic flow we use the physical data needed for determining the potential as they are obtained for the control point itself. For supersonic flow we assign the physical data of a neighbor auxiliary point H lying upstream to the control point P itself. In this way the

accuracy becomes correspondingly higher, as H comes closer to P. The continuity equation at P thus assumes the following forms depending on the type of flow:

$$M < 1 \qquad (\varrho u)_{xP} + (\varrho w)_{zP} = 0$$

$$M > 1 \qquad \left[(\varrho u)_H\right]_{xP} + \left[(\varrho w)_H\right]_{zP} = 0$$

## 5.2 Artificial Viscosity

For supersonic flow the described formulation can, using the values at the control point, be represented mathematically as a Taylor development which will first be demonstrated for $\varrho u$:

$$(\varrho u)_H = (\varrho u)_P + (\varrho u)_{Ps} (s_H - s_P)$$

The derivation $(\varrho u)_s$ is formed as follows:

$$(\varrho u)_s = (\varrho \frac{u}{q} q)_s = (\frac{u}{q})_s \varrho q + \frac{u}{q} (\varrho q)_s$$

Since we move along a stream line in the small interval $s_P$-$s_H$, its curvature plays no role so that $(\frac{u}{q})_s$ disappears.

$$(\varrho u)_H = \varrho u + \frac{u}{q} (\varrho q)_s \Delta s$$

The lowest arithmetical cost for a computer program is attained if, instead of s we introduce the density $\varrho$ as independent variable: /13

$$(\varrho q)_s \Delta s = (\varrho q)_\varrho \Delta \varrho = (q + \varrho q_\varrho) \Delta \varrho =$$

$$= (q + \frac{\varrho}{\varrho q}) \Delta \varrho = q (1 + \frac{\varrho}{q \varrho_q}) \Delta \varrho$$

With the aid of (10) we then obtain:

$$(\varrho q)_s \Delta s = q(1 - \frac{1}{M^2}) \Delta \varrho$$

The expression in parentheses is negative for subsonic flow and disappears exactly for sonic velocity so that for differentiating the type of flow we can introduce the switch function "max"

$$(\varrho u)_{II} = \varrho u + u \max\left\{0,\left(1 - \frac{1}{M^2}\right)\right\}\Delta\varrho$$

$$= \left[\varrho + \max\left\{0,\left(1 - \frac{1}{M^2}\right)\right\}(\varrho_{II} - \varrho)\right] u$$

Analogously:

$$(\varrho w)_{II} = \left[\varrho + \max\left\{0,\left(1 - \frac{1}{M^2}\right)\right\}(\varrho_{II} - \varrho)\right] w$$

Accordingly for transonic computer programs we need only replace the density by

$$\varrho \rightarrow \varrho + \max\left\{0,\left(1 - \frac{1}{M^2}\right)\right\}\Delta\varrho$$

The additional methodology is not affected thereby.

5.3 Viscosity Parameter /14

Since the length of the vector $\Delta s$ between auxiliary point H and control point P is fixed by the discretionary dimension of the mesh network on which the computer program is based, the viscosity is generalized by the parameter $\varepsilon$ .

$$\varrho \rightarrow \varrho + \varepsilon \max\left\{0,\left(1 - \frac{1}{M^2}\right)\right\}\Delta\varrho$$

Normally the value of $\varepsilon$ will be close to 1. On the one hand, for a large number of meshes, the accuracy can be increased by the selection of a decreased viscosity parameter, but on the other hand there is danger that no iterative convergence is attained if the value of $\varepsilon$ is too small. As shown by numerical experiments variations of $\varepsilon$ can displace the compression shock within an interval of about 5% of the airfoil height.

## 6. The Variation Principle

/15

### 6.1 Weighted Residuum

Since we do not know, ahead of time, the solution of the continuity equation (1) in conjunction with rotational freedom (12), (13), we have no choice except to introduce into it an approximating function with free parameters which must be chosen such that (1) is satisfied as well as possible. In this way the right side of equation (1) will generally not disappear exactly

$$(\varrho u)_x + (\varrho w)_z = R \neq 0$$

The remainder R is called the residuum.

There is a temptation to weight the residuum with a function in such a way that large residua are emphasized greatly while small residua are emphasized little and to demand that the integral thus formed disappear for the entire flow region. Such a weighting function is surely a deviation of the approximating potential distribution from the exact $\phi$ :

$$\iint R\ (\phi - \bar{\phi})\ dx\ dz = 0$$

Here, however, $\phi$ is unknown. However one can, under the assumption that $\bar{\phi}$ deviates only little from the exact distribution, approximate the exact $\phi$ values by the linear Taylor expansion:

$$\phi = \bar{\phi} + \bar{\phi}_\phi\ (\phi - \bar{\phi})$$

Introduce

$$\iint R\ \bar{\phi}_\phi\ (\phi - \bar{\phi})\ dx\ dz = 0$$

Little seems to be gained in this way since the unknown exact solution is still contained therein. However, the disappearance of the integral can still be guaranteed if we demand that

$$\iint R\ \bar{\phi}_\phi\ dx\ dz = 0$$

With (1), (12), (13) the following should then be true /16

$$\iint \left[ (\varrho \bar{\varphi}_x)_x + (\varrho \bar{\varphi}_z)_z \right] \bar{\varphi}_\phi \, dx \, dz = 0$$

Here, analogously to (18) partial integration can be used if we make the formal substitution:

$$e \longrightarrow \bar{\varphi}_\phi$$

$$\varphi_x \rightarrowtail \varrho \bar{\varphi}_x, \quad \varphi_z \rightarrowtail \varrho \bar{\varphi}_z$$

$$\oint_C \bar{\varphi}_\phi \varrho \, \varphi_n \, ds - \iint_{(B)} \varrho \left[ \bar{\varphi}_x \bar{\varphi}_{\phi x} + \bar{\varphi}_z \bar{\varphi}_{\phi z} \right] dx \, dz = 0$$

The first integral disappears since the mass-flux integral over the exterior boundary far downstream of the airfoil must be zero according to definition and since the fluid cannot penetrate the profile contour. If we interchange the differentiation in the second integral and write as in (12), (13), then we reach the remarkably simple result

$$\iint \varrho (u u_\phi + w w_\phi) \, dx \, dz = 0$$

Thus the contour boundary condition is implicitly contained therein.

6.2 Minimum pressure integral

Equation (23) can be further simplified. With (8) we get to

$$\frac{1}{2} \iint \varrho q^2_\phi \, dx dz = \frac{\varrho_0}{2} \iint \left(1 - \frac{\varkappa - 1}{2} q^2\right)^{\frac{1}{\varkappa - 1}} q^2_\phi \, dx dz =$$

$$= - \frac{\varrho_0}{\varkappa} \iint \left(1 - \frac{\varkappa - 1}{2} q^2\right) \frac{\varkappa}{\varkappa - 1} \varphi_\phi \, dx dz = 0$$

The integrand is identified with (4) as a normalized pressure:

$$\iint p_\phi \, dx \, dz = 0$$

This result can be confirmed in a simple manner from the principle of energy minima in closed systems. Imagine that a very large plate is dragged through a flow field where one side is subjected to the static pressure p of the flow while a constant equalization pressure is in effect on the back side. For the sake of simplicity let us assume that

the plate is mounted vertically and that the drag direction is horizontal. Then the work associated with the drag is

$$A = \int K \, dx = b \iint (p - \text{konst}) \, dz \, dx$$

The minimum principle demands that $A = A_{min}$, thus

$$\iint (p - \text{konst}) \, dx \, dz = \text{Min}$$

or

$$\iint c_p \, dx \, dz = 0$$

The result of this is that an exact minimum is never attained when an approximation is introduced. The pressure thus is overestimated while the velocity is underestimated.

## 7. Numerical Evaluation /18

### 7.1 Choice of Element

For the evaluation of (23) we require a stepwise approximation of the potential using free parameters which must be determined such that the value of the integral (23) disappears. This is customarily done by the method of finite elements. In deriving the minimum principle we started with the idea that the potential approximation does not deviate much from the exact solution. In contrast to the non-sensical convergence criteria often cited in the basic literature we state here precisely that:

- The elements must be laid out in such a way that they always furnish the potential distribution.

- For constant density the element must be source free:

$$\rightarrow \oint \phi_n \, ds = 0$$

for all closed contours lying within the element including the boundary. This is the same as

$$\phi_{xx} + \phi_{zz} = 0$$

Therefore the density does not have to be considered because, as the size of the element becomes infinitely small, it can be placed as a constant in front of the through-flow integral.

- The element must have at least enough free parameters so that the validity of the continuity equation in integral form can be assured, without contradiction, for any closed control contour.

Except for the area panel [1], [2] known in theoretical aerodynamics there is no element which satisfies the above requirements. Since it has not been possible to date to incorporate the area panel into transonic computer programs, there is no other choice except to try to find, by trial methods, one of the known classical elements which comes closest to satisfy the engineering demands. /19

a. The linear triangle

although with the equation

$$\phi = a + bx + cz$$

it satisfies the continuity equation trivially, it does not satisfy the third convergence condition. One can easily see this, if somewhere in the flow field a velocity vector $\vec{q}$ and a single potential value $\phi_o$ is fixed. This is always possible by a proper choice of the constant of integration.

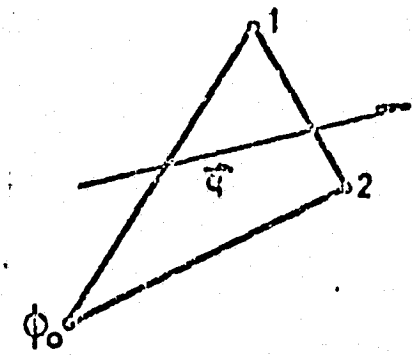

In this way the potential values in 1 and 2 are known. We now add another triangle 1-2-3:

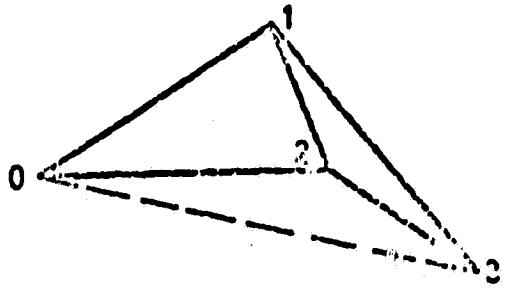


If we set the mass flux at the separating line 1-2 equal on both sides, then we obtain the value $\phi_3$. If we complete the triangle configuration with the indicated side 3-0, then the mass flux condition via 2-3 no longer furnishes the value $\phi_0$. The forced juncture-coupling of the triangles among each other leads to a redundancy. /20

Figure 1 shows as an example a shock-free NLR airfoil which was subsequently calculated with this element. As expected, the result is, as predicted, unusable, figure 2.

The mutual coupling is cancelled only in the special case of right angle, isosceles triangles and the influence matrix for the potential values degenerates to that of the difference scheme. If the triangles are not isosceles, then 2 triangle sides must always coincide with a potential line and a stream line in order to achieve an exact convergence solution.

Although Shen [3] and Habashi [4] report useful results with this element, they knowingly or unknowingly deceive the reader because the airfoil is first transformed into a near circular, conformal image plane where a nearly orthogonal network is constructed which additionally follows approximately the $\phi$- resp. the $\psi$- lines. For non- orthogonal networks their methods are useless.

Brashears and Chan[5] work directly in the plane of flow and can give only a rather challengeable interpretation of their weak results. Although Periaux and Perrier [6] write a lot of theory, they produce no significant sensible results.

b. The quadratic triangle

/21

is based on the expression

$$\phi = a + bx + cz + dxz + ex^2 + fz^2.$$

Here the second convergence requirement is generally violated. The Laplace equation is satisfied only if $e = -f$. This again is only true if the elements are arranged in a rectangular network. By an expansion to 6 parameters the juncture-coupling is only apparently cancelled completely. In reality the juncture axes are now curved so that the redundancy is reduced, but still noticeable. For a method using this element the computer time is unjustifiably large. The unusable result shown in figure 3 requires, e.g., 25 minutes on the central computer of an IBM 360/168.

c. The four-point quadrangle element

is decidedly the best element. In a quadratic orthogonal combination the matrix degenerates to the difference scheme in the network rotated by 45° for that purpose.

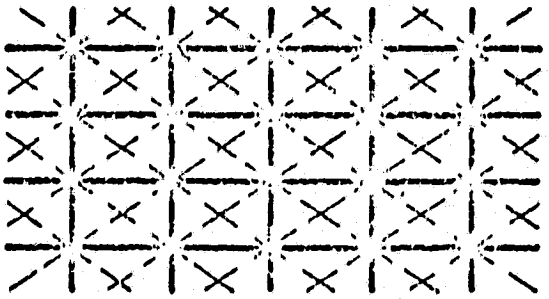

In a right angle-quadrilateral combination the Laplace equation is satisfied exactly everywhere. For an arbitrary element shape the Laplace equation is at least satisfied at the Thales circle via both radiating points. /22

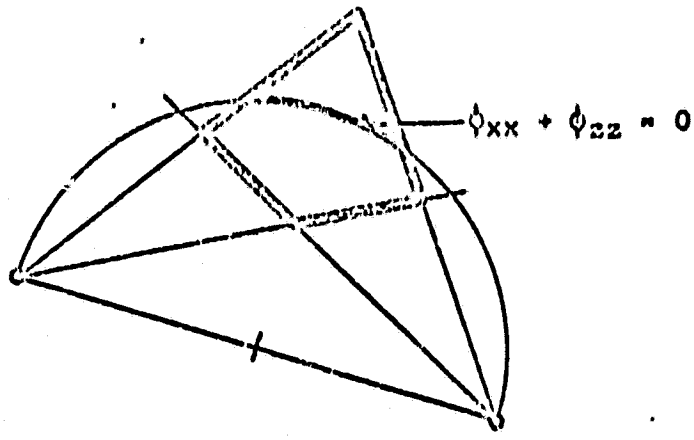


There is no redundancy. This element does not conform to the convergence criteria found in the text books, which incidentally are wrong; therefore it is seldom used, but satisfies the requirements listed here if the elements are distributed in such a way that the basic circles intersect the elements associated with them.

d. The eight-pointed quadrangle element

is not as good as the four-pointed one since the matrix-diagonal elements for the corner points disappear exactly in the quadratic combination or otherwise are smaller than the neighboring elements so that the resulting system of equations for the potential values is conditioned extremely poorly.

Hirsch [7] also reports relaxation factors smaller than 0.25 so that we cannot consider this element. For a quadratic network division that author's method would fail for successive network refinement.

## 7.2 The bilinear square



As a basic area for the approximation of a function f let us use a square of the following design:

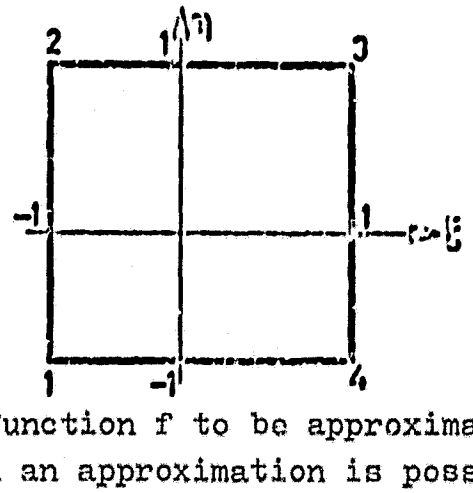


Let us say that the function f to be approximated is known at the corners 1 to 4. Then an approximation is possible for the values of the function on the inside and at the edges of the square by using the expression

$$f = a + b\xi + c\eta + d\xi\eta.$$

The coefficients are to be determined so that the polynomial takes on the exact values of the function at the corners:

$$f_1 = a - b - c + d$$
$$f_2 = a - b + c - d$$
$$f_3 = a + b + c + d$$
$$f_4 = a + b - c - d$$

Since the system of equations is nearly decoupled, the solution is simplified and after trivial rearrangements leads to the following result:

$$f = \frac{1}{4}\,[f_1 (1-\xi)(1-\eta) + f_2 (1-\xi)(1+\eta) + f_3 (1+\xi)(1+\eta) + f_4 (1+\xi)(1-\eta)]$$

By abbreviating we obtain the following /24

$$f = \sum_{1}^{4} f_1 G_1$$

where $G_1$ is called the form function.

## 7.3 The quadrangle_element

The specialized results from the preceding section can easily be carried over to a general quadrangle if this is transformed to the image square by means of the so-called isoparameters. This is done by identifying f successively as follows:

$$\phi = \sum_{1}^{4} \phi_1 G_1 \qquad (24)$$

$$x = \sum_{1}^{4} x_1 G_1 \qquad (25)$$

$$z = \sum_{1}^{4} z_1 G_1 \qquad (26)$$

However, in the present minimization method the potential distribution itself is not needed, but rather their derivations in the x- and z- directions:

$$\phi_x = \phi_\xi \xi_x + \phi_\eta \eta_x$$
$$\phi_z = \phi_\xi \xi_z + \phi_\eta \eta_z$$

Now $\xi$ and $\eta$ cannot be inverted simply to functions of x and z so that we must first find the distortion determinant as a function of $\xi$ and $\eta$ . Here we write the total differential as:

/25

$$d\xi = \xi_x\, dx + \xi_z\, dz$$
$$d\eta = \eta_x\, dx + \eta_z\, dz$$
$$dx = x_\xi\, d\xi + x_\eta\, d\eta$$
$$dz = z_\xi\, d\xi + z_\eta\, d\eta$$

If we insert the upper two equations into the expressions for dx and dz, then we obtain

$$dx = (x_\xi \xi_x + x_\eta \eta_x)dx + (x_\eta \eta_z + x_\xi \xi_z)dz$$
$$dz = (z_\xi \xi_x + z_\eta \eta_x)dx + (z_\eta \eta_z + z_\xi \xi_z)dz$$

dx must be independent of dz so that by exchanging coefficients we obtain four equations:

$$x_\xi \xi_x + x_\eta \eta_x = 1$$
$$x_\eta \eta_z + x_\xi \xi_z = 0$$
$$z_\eta \eta_z + z_\xi \xi_z = 1$$
$$z_\xi \xi_x + z_\eta \eta_x = 0$$

Solving for the unknowns $\xi_x$, $\xi_z$, $\eta_x$, $\eta_z$ we get

$$\xi_x = \frac{z_\eta}{D} \qquad (27)$$

$$\xi_z = -\frac{x_\eta}{D} \qquad (28)$$

$$\eta_x = -\frac{z_\xi}{D} \qquad (29)$$

$$\eta_z = \frac{x_\xi}{D} \qquad (30)$$

with $D = x_\xi z_\eta - x_\eta z_\xi$ (31)

Thus all operations for the formation of the functional relations have been prepared.

## 7.4 Energy of the element

/26

The term element energy is defined as the value of the integral (23) over the element. As a pivotal point we choose the corner 1. In order to keep the computer cost as low as possible we assume that the density is constant as distributed over the element. Using

the chain rule of differentiation we obtain, with equations (27) to (31) the following expression for the element energy:

$$I = \varrho \sum_{1}^{4} \phi_i \int_{-1}^{1}\int_{-1}^{1} \Big\{ G_{1\xi} \big[ z_\eta (G_{1\xi}\, x_\eta - G_{1\eta}\, x_\xi) - \quad (32)$$
$$x_\eta (G_{1\eta}\, x_\xi - G_{1\xi}\, x_\eta) \big] +$$
$$G_{1\eta} \big[ x_\xi (G_{1\eta}\, x_\xi - G_{1\xi}\, x_\eta) -$$
$$x_\xi (G_{1\xi}\, z_\eta - G_{1\eta}\, z_\xi) \big] \Big\} \frac{d\xi\, d\eta}{b}$$

## 7.5 Numerical integration

It is extremely difficult to determine the value of the integral (23) in an elementary manner. Therefore one tries to find at least a good approximation value using Gaussian integration. For the one-dimensional integral we first form the expression

$$\int_{-1}^{1} f\, d\xi = a\, f(\xi_1) + b\, f(\xi_2)$$

This formula should be exact for the four test functions

$$f_n = \xi^n \quad (n = 0, 1, 2, 3)$$

Then the following is true

/27

$$n = 0 \qquad \int_{-1}^{1} d\xi = 2 = a + b$$

$$n = 1 \qquad \int_{-1}^{1} \xi d\xi = 0 = a\xi_1 + b\xi_2$$

$$n = 2 \qquad \int_{-1}^{1} \xi^2 d\xi = \frac{2}{3} = a\xi_1^2 + b\xi_2^2$$

$$n = 3 \qquad \int_{-1}^{1} \xi^3 d\xi = 0 = a\xi_1^3 + b\xi_2^3$$

The thus resulting system of equations for the four unknowns $a$, $b$, $\xi_1$, $\xi_2$ can be solved in a simple way and leads to the following result

$$a = b = 1$$

$$\xi_1 = -\frac{1}{\sqrt{3}}$$

$$\xi_2 = \frac{1}{\sqrt{3}}$$

Thus for the general integral the following is true:

$$\int_{-1}^{1} f\, d\xi = f\left(-\frac{1}{\sqrt{3}}\right) + f\left(\frac{1}{\sqrt{3}}\right)$$

The double integral can be evaluated as an approximation by means of 2-fold Gaussian quadratics:

$$I = \int_{-1}^{1}\int_{-1}^{1} f\, d\xi\, d\eta = \int_{-1}^{1}\left[f\left(-\frac{1}{\sqrt{3}},\eta\right) + f\left(\frac{1}{\sqrt{3}},\eta\right)\right] d\eta =$$

$$= f\left(-\frac{1}{\sqrt{3}},-\frac{1}{\sqrt{3}}\right) + f\left(-\frac{1}{\sqrt{3}},\frac{1}{\sqrt{3}}\right) + f\left(\frac{1}{\sqrt{3}},\frac{1}{\sqrt{3}}\right) + f\left(\frac{1}{\sqrt{3}},-\frac{1}{\sqrt{3}}\right)$$

## 7.6 Stiffness matrix

/28

### 7.6.1 Field-point collocation

Until now the special corner 1 of an element was chosen as the starting point for the element energy. It is understood that in a global element combination the four elements coming together at a point furnish a contribution to the integral (23). Here (32) is considered to be unchanged if the element corner numbering system is retained locally by a corresponding rotation of the coordinates:

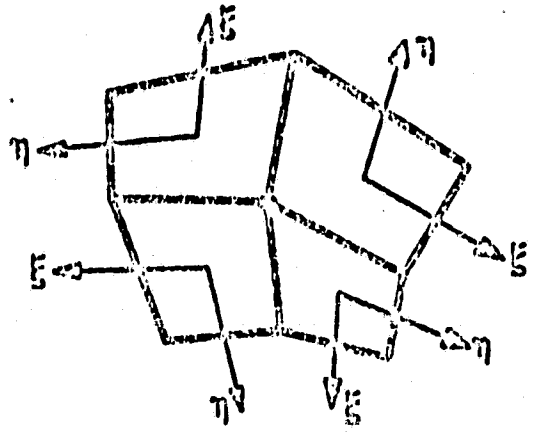


Since we use column relaxation in the computer program, instead of the entire stiffness matrix we need only build up the tri-diagonal matrix for a selected line. The contributions of discretionary points which are not located on this line, are placed on the right-hand side of the system of equations:

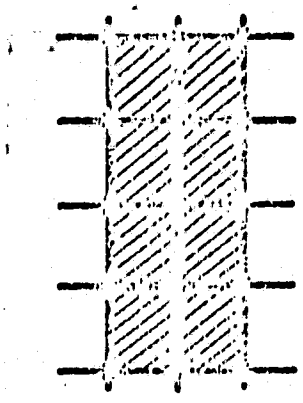

o matrix contribution

x right-hand side

7.6.2 Boundary_point_collocation

/29

At the extreme boundary of the computer network the potential values are assumed for the far-field solution (16), (20), (21)

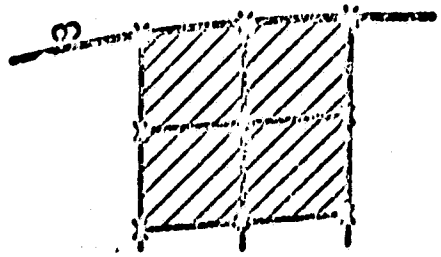

o matrix contribution
x right-hand side

At the boundary of the airfoil obviously only two instead of four elements contribute to the formation of the column matrix:

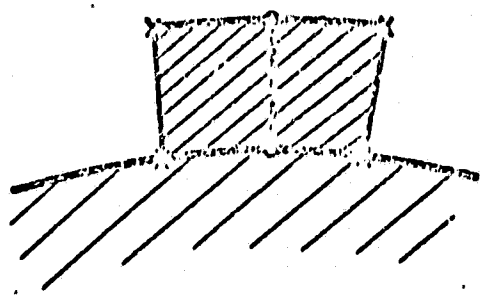

7.6.3 Circulation-slot_collocation

/30

To determine the circulation $\Gamma$ for equation (21) the potential values the potential values are calculated directly according to (22), after each field relaxation, at the upper and lower surface of the trailing edge of the airfoil.

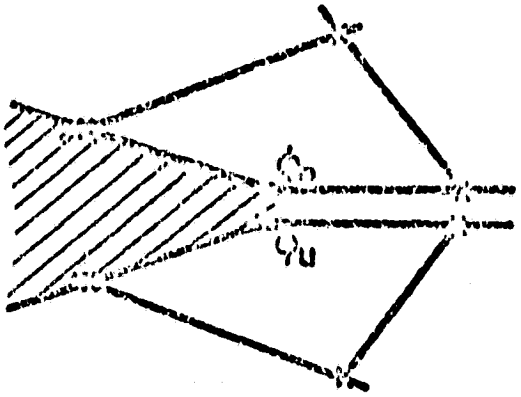


For the slot itself we make use of (22) and, e.g., replace $\phi_o$ with $\phi_u + 2\pi\Gamma$. Only then can the derivation be carried out according to (23) from the potential values of the lower bank. As in field collocation, the contributions of four elements each constitute a pivotal value. The contributions of the element energy which were multiplied by $\Gamma$ are transposed to the right-hand side of the tri-diagonal matrix:

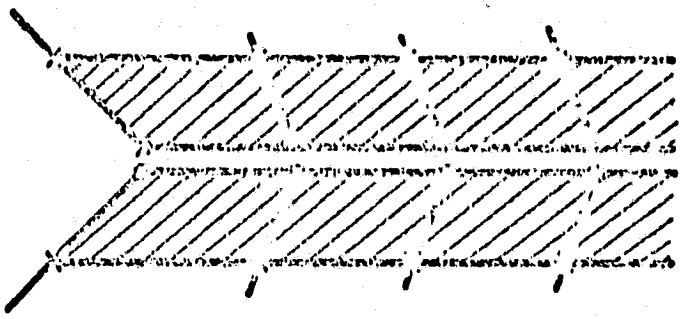

o matrix contribution

x right-hand side

## 8. Results

/31

- NLR Lifting Airfoil

As already mentioned, not all elements give the same results. The disadvantages of the linear triangle have already been discussed. Thus it is only necessary to look at figures 1 and 2 to discover that this element cannot be used.

For similar reasons the quadratic triangle also fares poorly in the numerical comparison, figure 3.

As an experiment the quadrangle element was tested to see if it could satisfy the continuity equation in a conservative manner. As shown in figure 4 the pressure is greatly underestimated. A similar procedure is suggested by Jameson and Caughey [11], who, however, seem to obtain usable results. Through refinement of the network the mentioned effect is enhanced, figure 5. Only the quadrangle element in conjunction with the principle of variations produces a satisfactory result, figure 6.

- NACA 0012

To accelerate convergence the following steps were taken:

- direction of relaxation = main stream direction
- excess relaxation of 180% for
- intensive subdivision of the network

/32

A series of networks and results is shown in figures 7 to 16.

For a transition to whatever network follows the potential distribution is interpolated linearly. The mesh buidup is controlled by the parameters and, of course, is done automatically.

The end result, figure 16, is not satisfactory since the viscosity parameter was chosen too small by 80%. For 100% the strength of the shock becomes realistic, figure 17.

- NACA 64A410

  This result is in good agreement with those in standard publications, figure 18.

- Whitcomb airfoil, figure 19

  The profile generated automatically according to [9] was to show to what degree strong "rear loading" is reproduced. Here we must point out the necessity for Gaussian integration to obtain the element energy. The version of the program using trapezoidal integration fails for this example.

- Korn airfoil

  Figure 20 points out the importance of the viscosity parameter. Although the solution does converge, the viscosity parameter for this highly sensitive profile must be set at 200% in order to dampen out the waviness in the supersonic region, figure 21; this is an indication that the method performs too "stably" so that, by increased viscosity, the correct root can be found from the many possibilities of the differential equations. /33

As the result of the steps taken to accelerate convergence the computer times are comparatively small. After 20 iterations on the last network the pressure distribution was entirely frozen.

This produced computer times for the central unit of an IBM 360/168

1 minute for the 62 . 16 network

4 minutes for the 124 . 32 network

## 9. Summary



With the introduction of a special method of finite elements in conjunction with the mathematical model of artificial viscosity it has been possible to produce a usable computer method for transonic flow around airfoils which does not require an orthogonal computer network so that the method can, in a simple manner, be adapted to three-dimensional disturbance problems. Such a program is in a test stage at the present time.

## REFERENCES


[1] Eberle, A. An exact hodograph method for the design of a supercritical profile
MBB-UFE 1168(0) 1975

[2] Stricker, R. On an integral equation method for calculation of the fully nonlinear potential flow about arbitrary section shapes
Euromech, Braunschweig 1976

[3] Shen, S.T. An aerodynamicist's looks at the finite element method
Finite Elements in Fluids Chap. 10 1975

[4] Habashi, W.G. The finite element method in subsonic aerodynamics
ZLDI CONF. 76-142-018 1976

[5] Brashears, M.R. and Chan, S.T.K. Finite element analysis of unsteady transonic flow
AIAA Paper No. 75-875 1975

[6] Perrier, P. and Periaux, J. Application of the finite element method in nonlinear aerodynamics
Karman Institute for Fluid Dynamics
Lecture Series 87 1976

[7] Hirsch, Ch. Introduction to the finite element method and its application in fluid dynamics
Karman Institute for Fluid Dynamics
Lecture Series 87 1976

[8] Eberle, A. Profile optimization for transonic flow
MBB-UFE-AERO-MT-304 1977

[9] Eberle, A. Profile definition program following the Whitcomb revelation report
MBB-UFE-AERO-MT-298 1977

[10] Eberle, A. ZKF cooperative effort
MBB-UH: Mass-flux method
1. profile optimization
2. method of finite elements for transonic flow past airfoils
MBB-UFE-AERO-MT-285 1977

[11] Jameson, A. and Caughey, D.A. A finite volume method for transonic potential flow calculations
AIAA Paper No. 77-635 1977

UFC1352

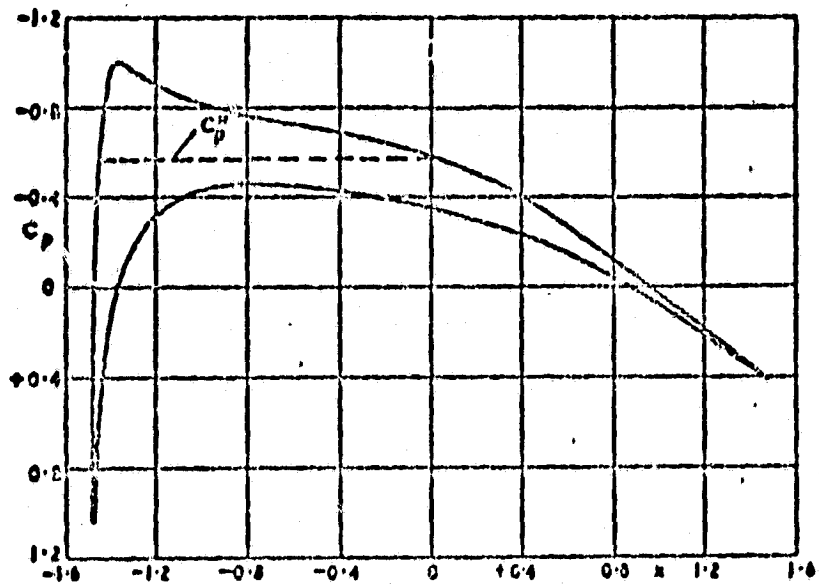


$\alpha = 1{\cdot}52^\circ$ $M_\infty = 0{\cdot}7557$



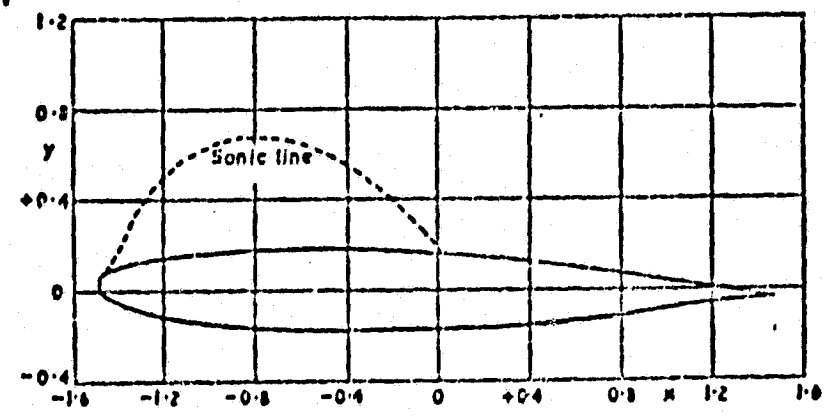


NLR lifting aerofoil (t/c = 0·121)

ABB. 1

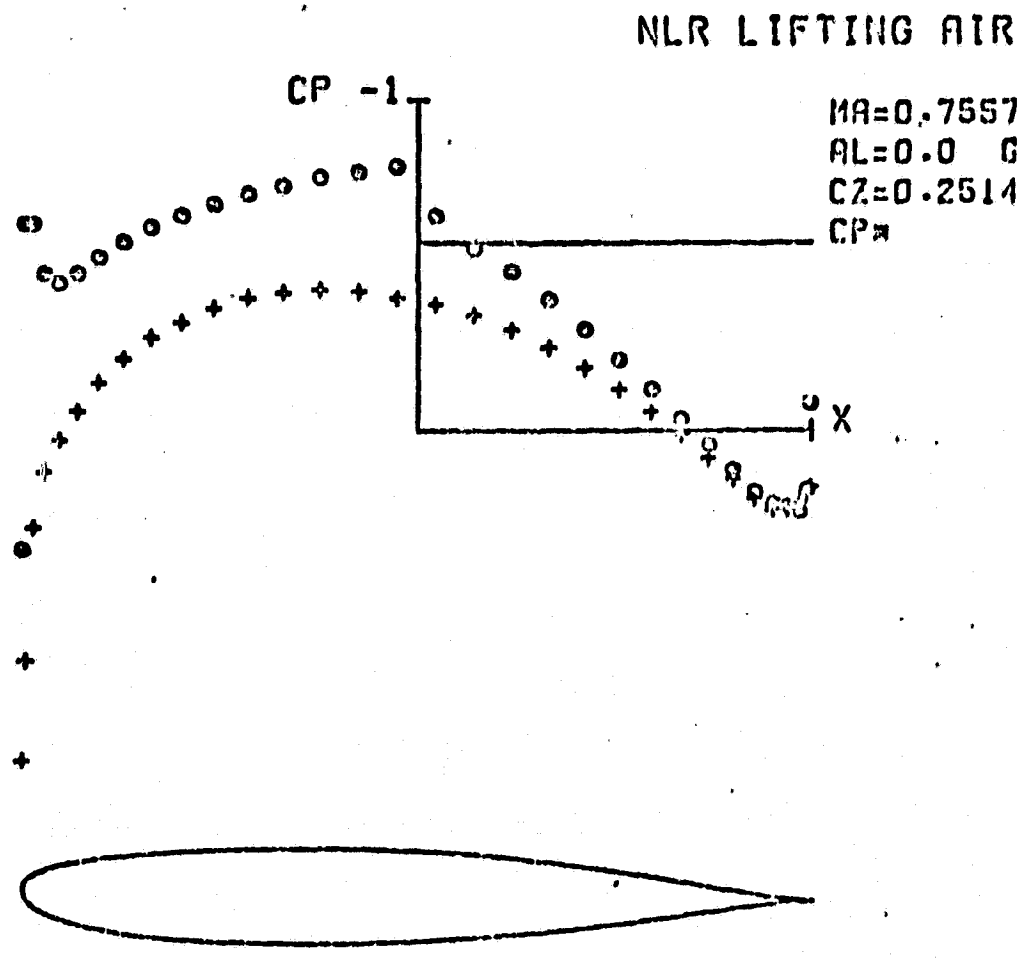


ABB. 2

UFE1352

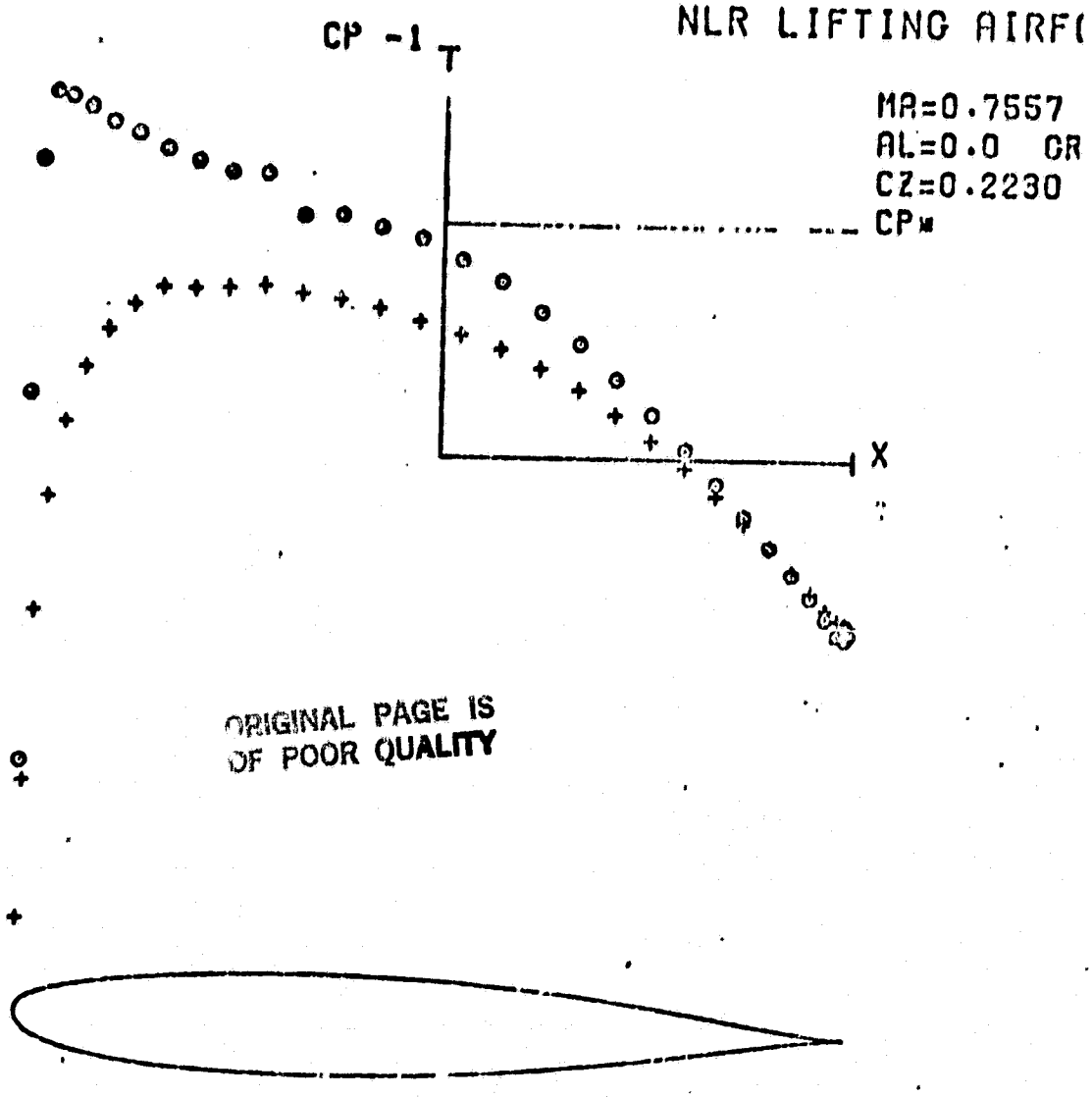




ABB. 3

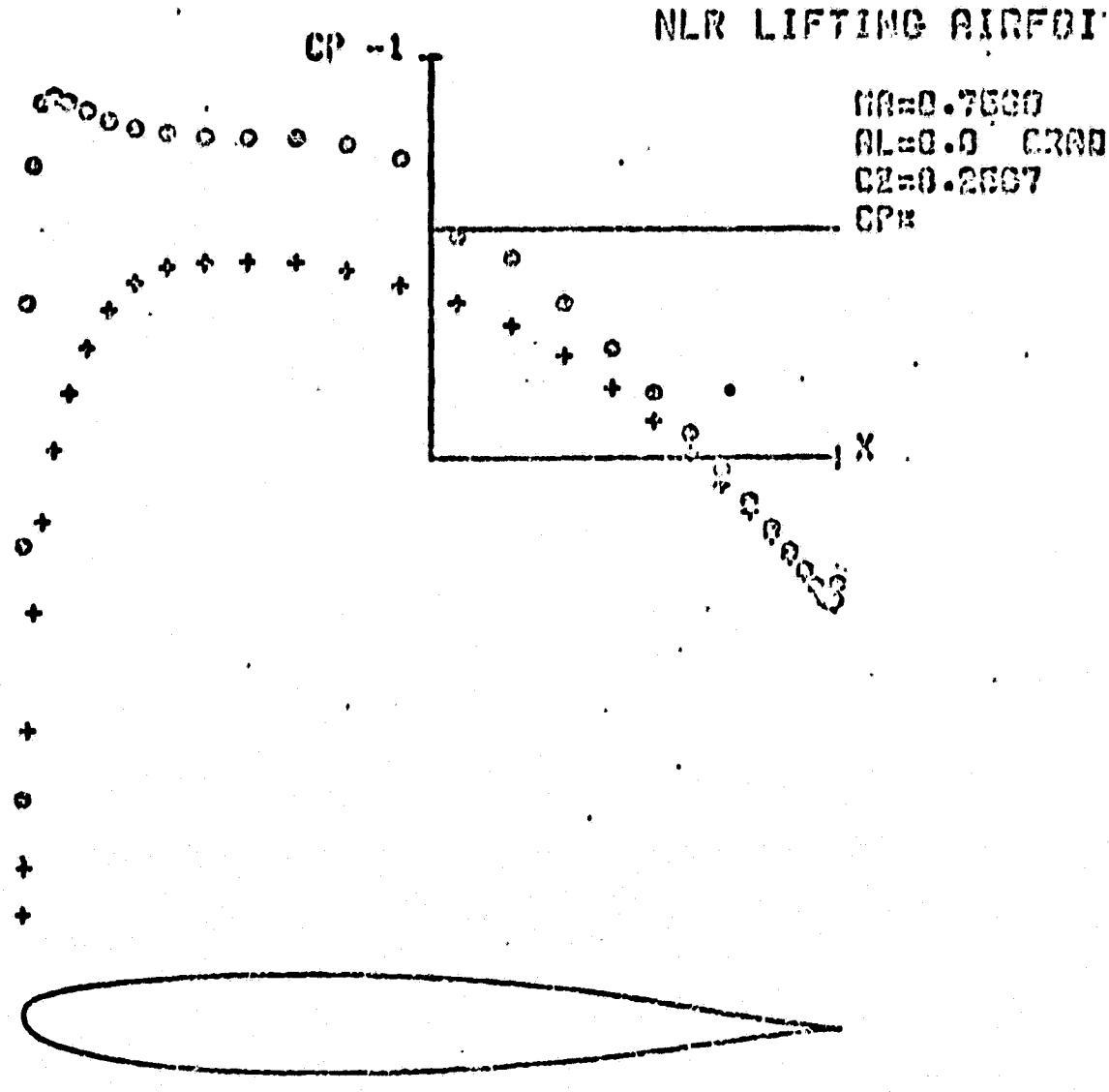


ABB. 4

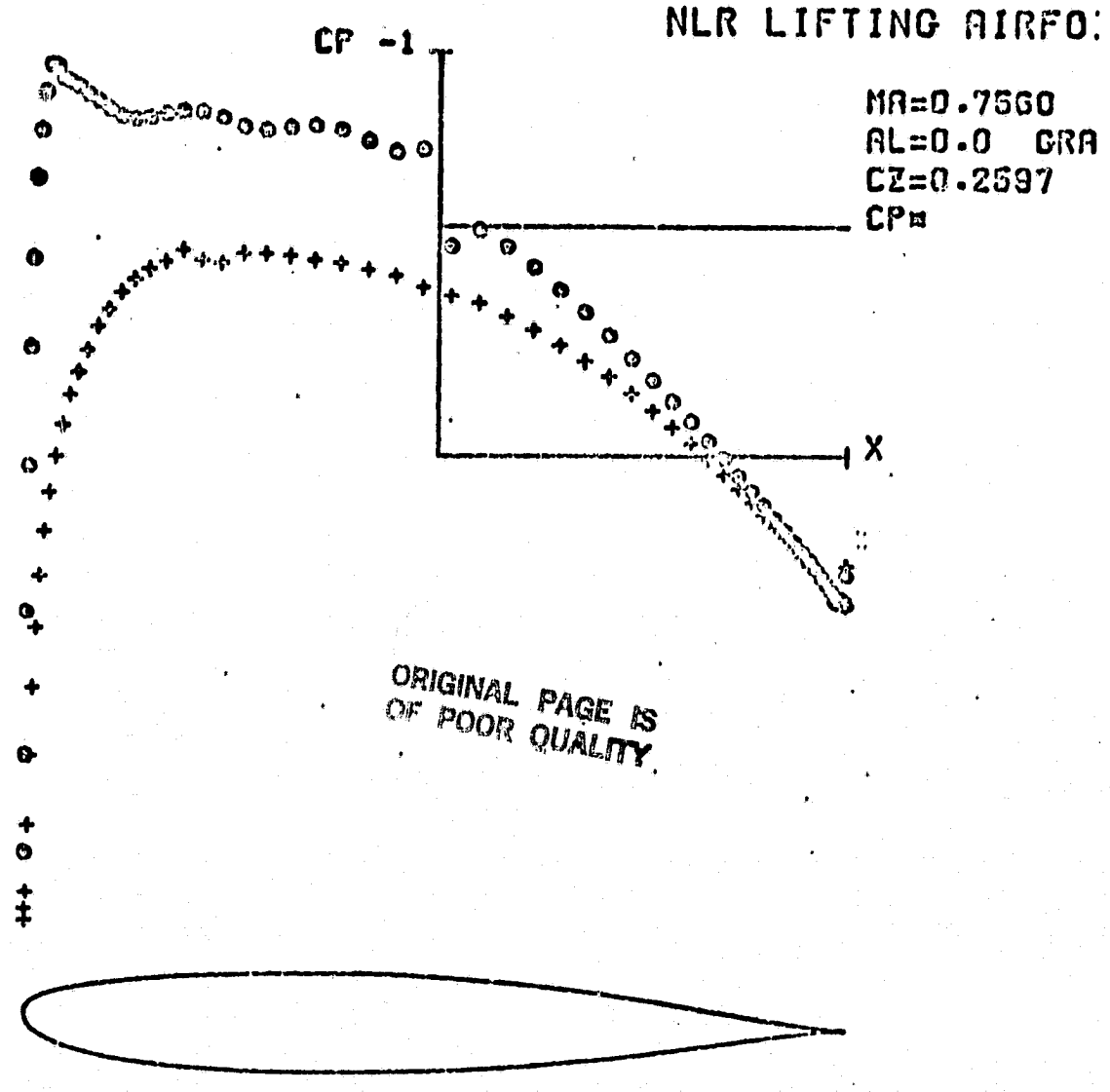




ABB. 5

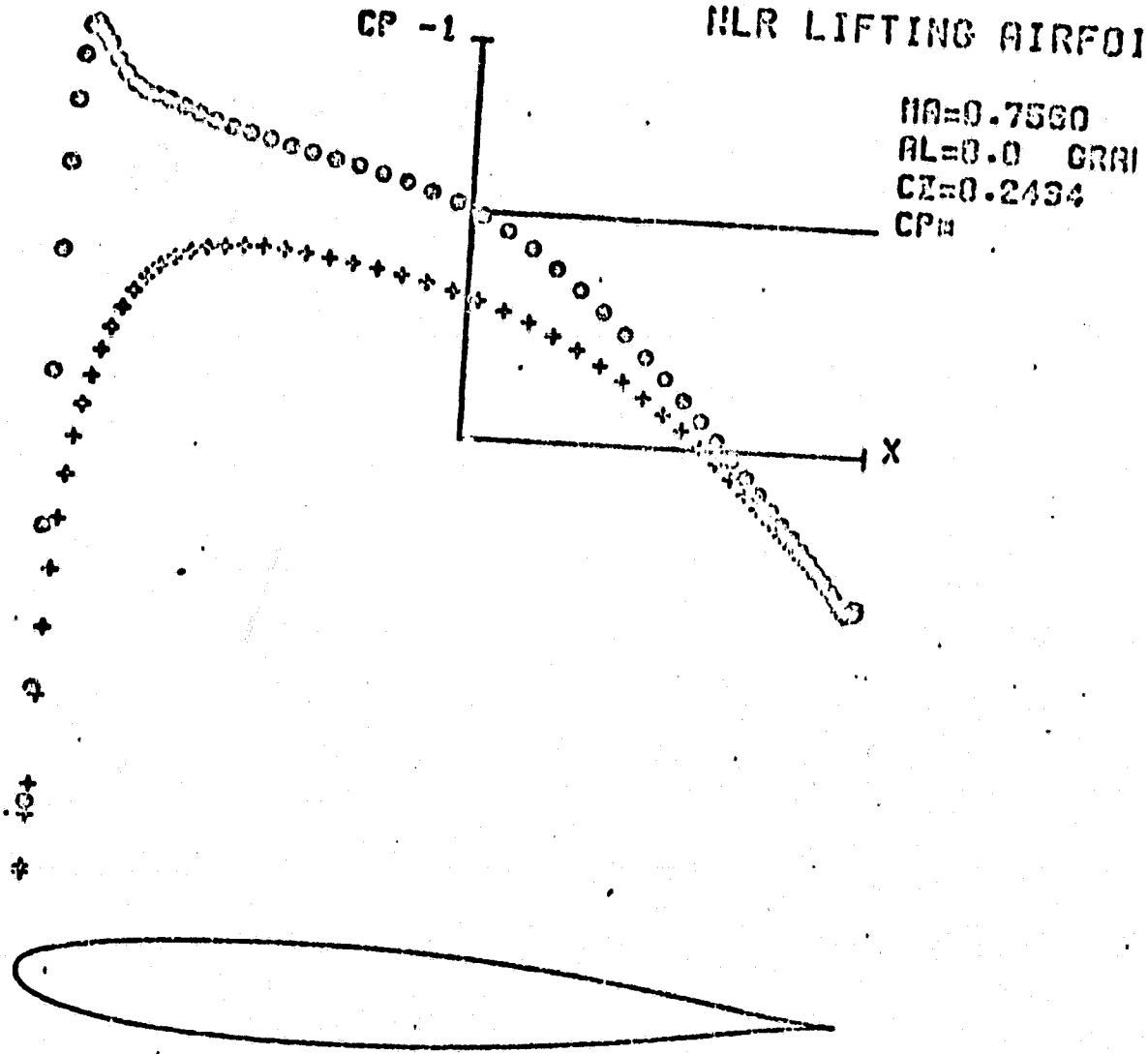


ABB. 6

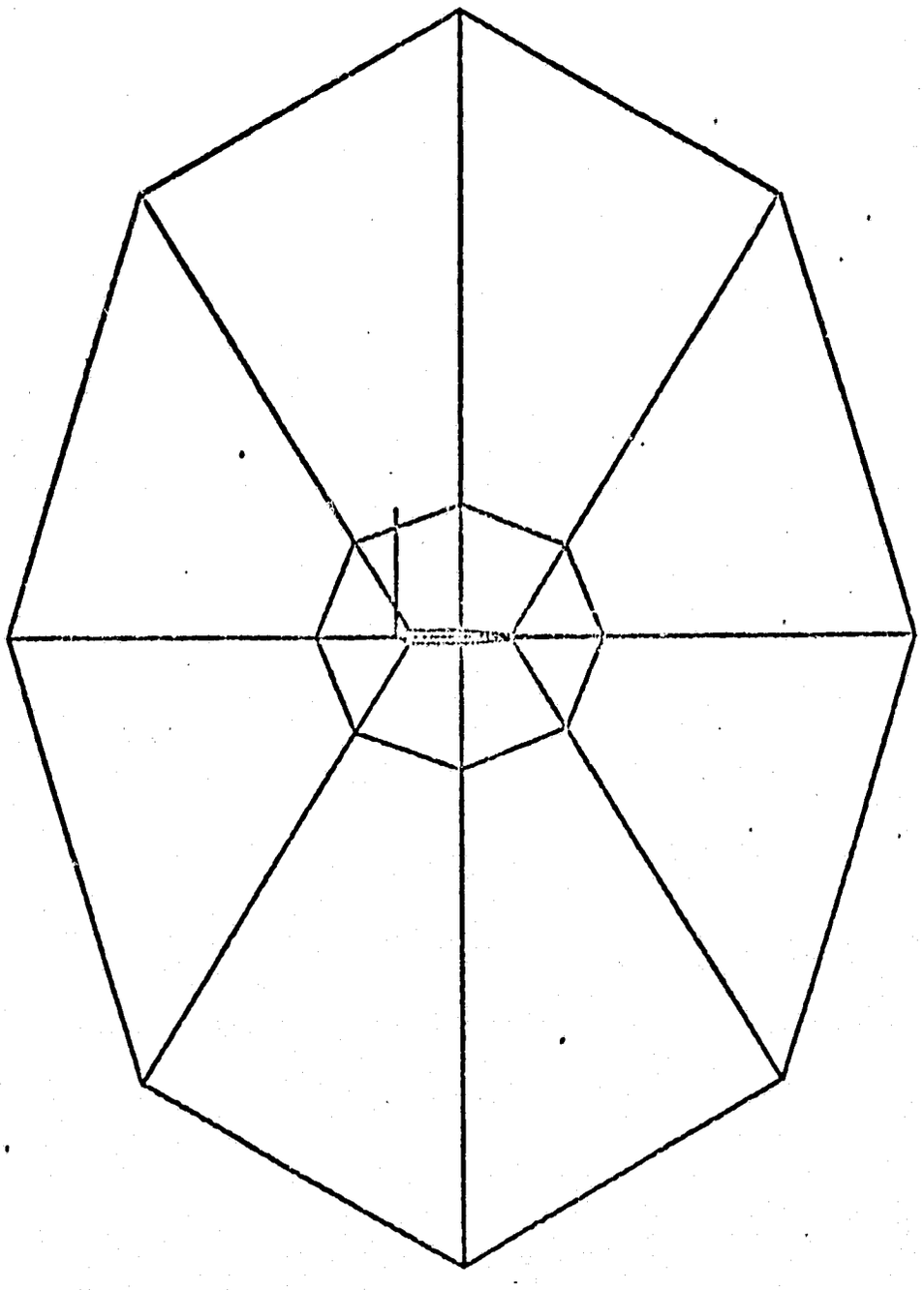

ABB. 7

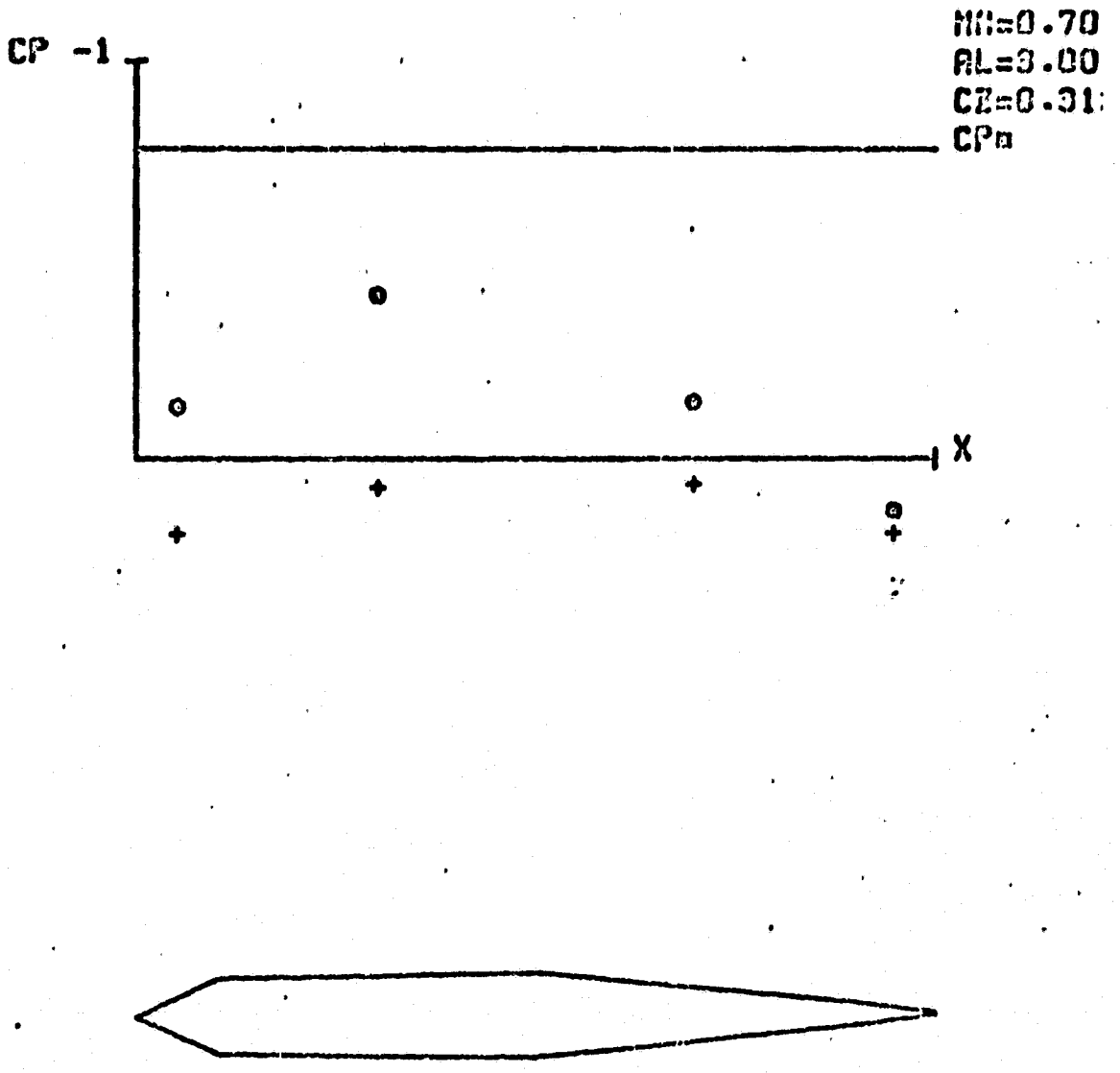


NACA 0012

ABB. 8

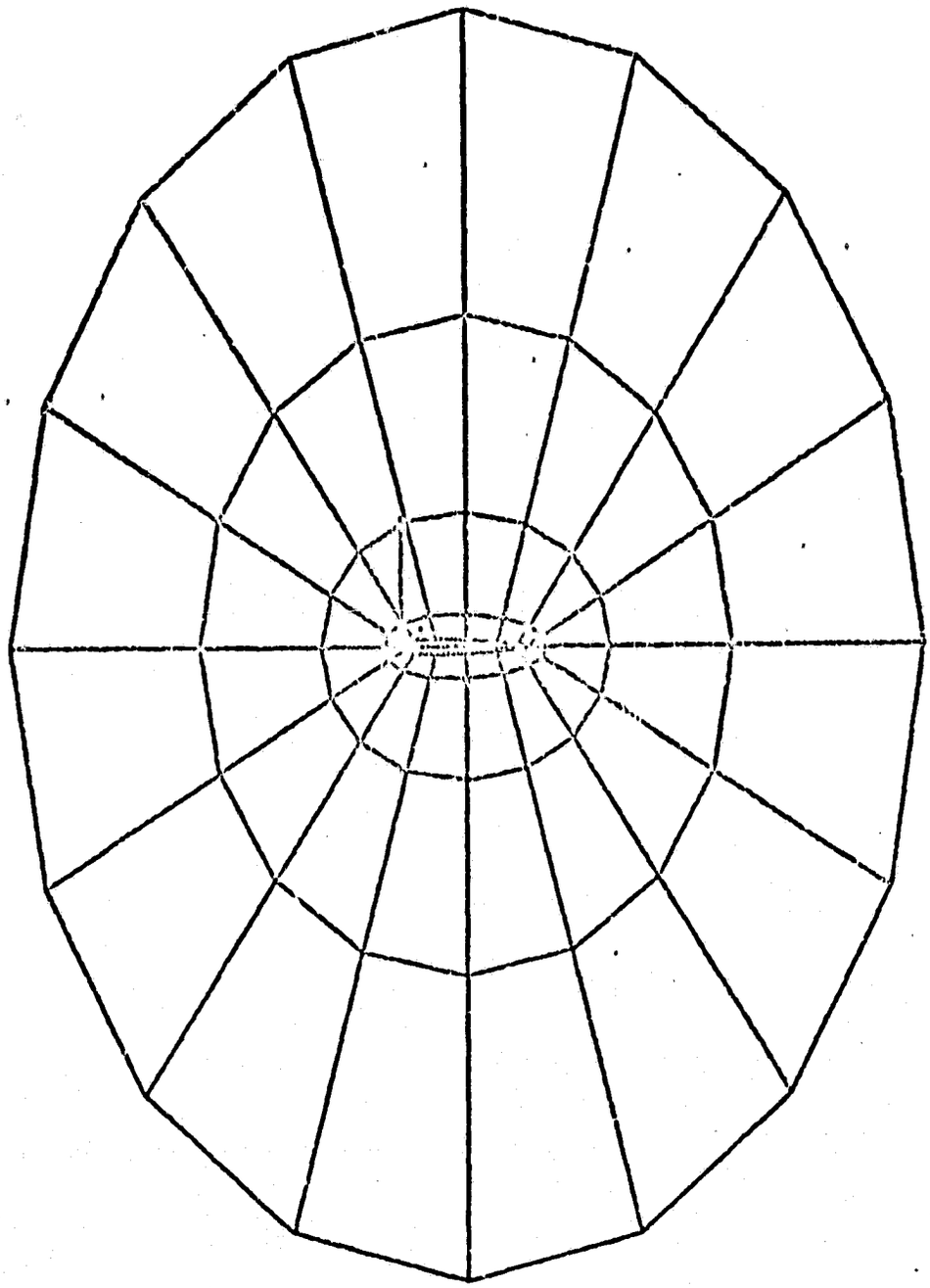

ABB. 9

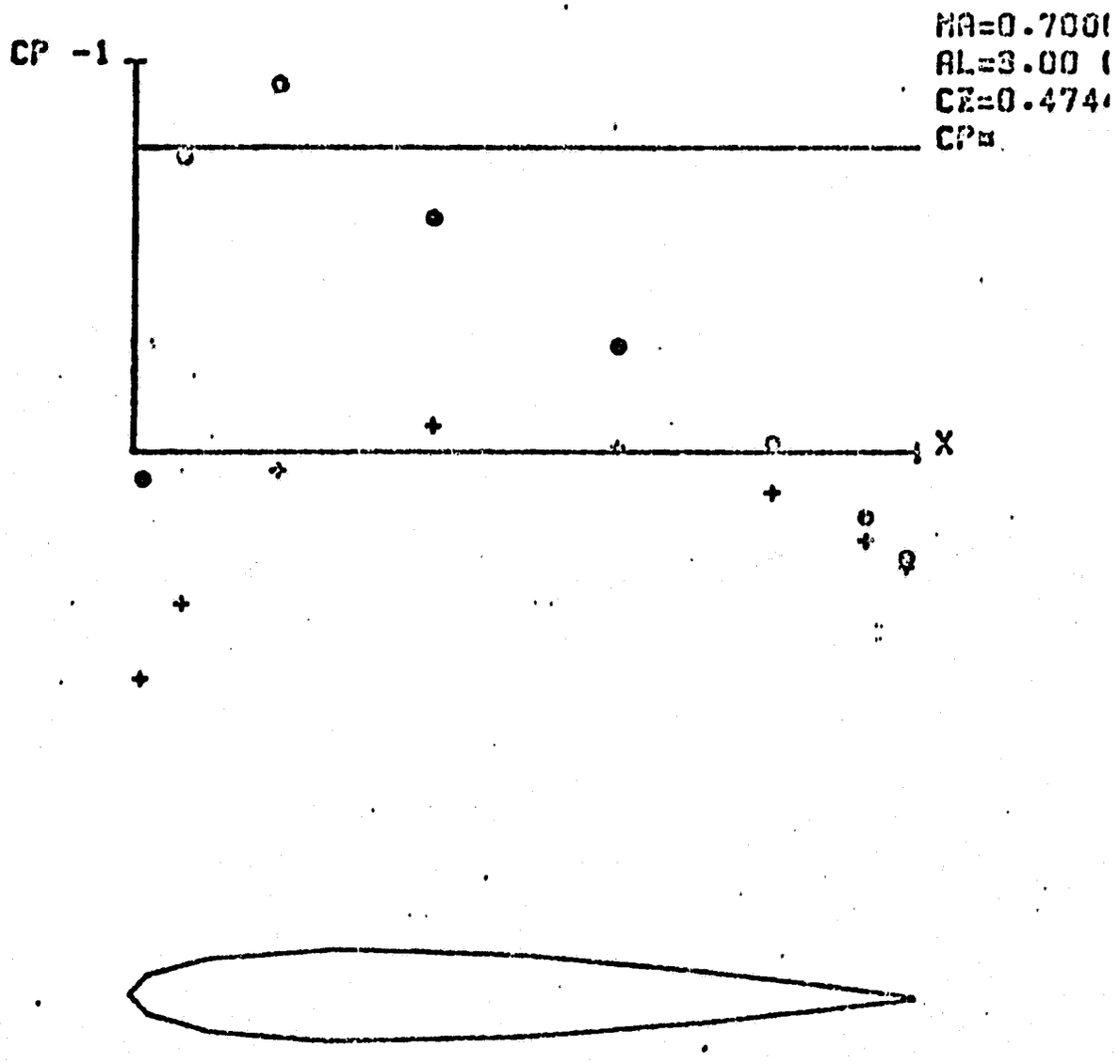


NACA 0012

ABB. 10

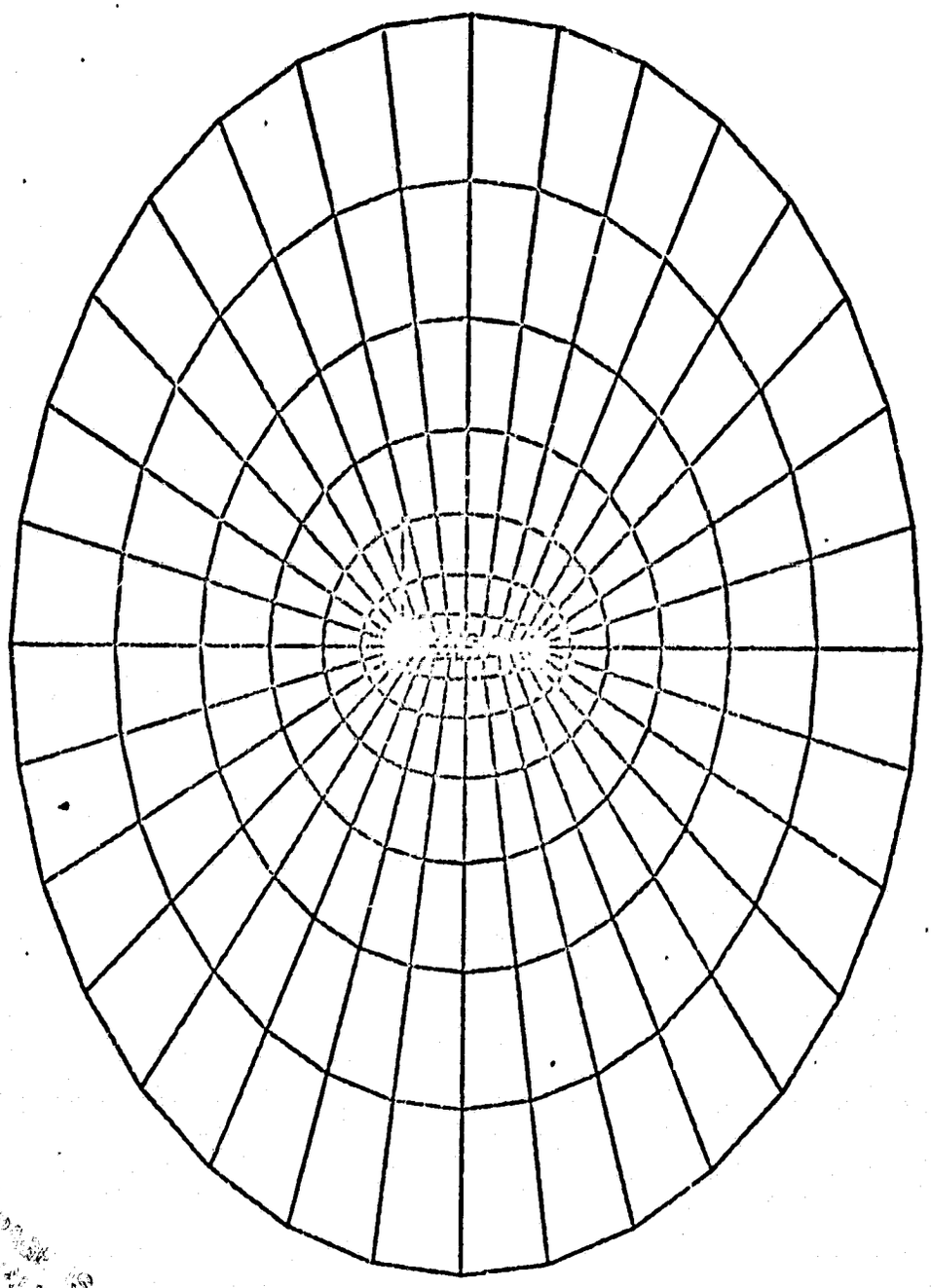

ABB. 11

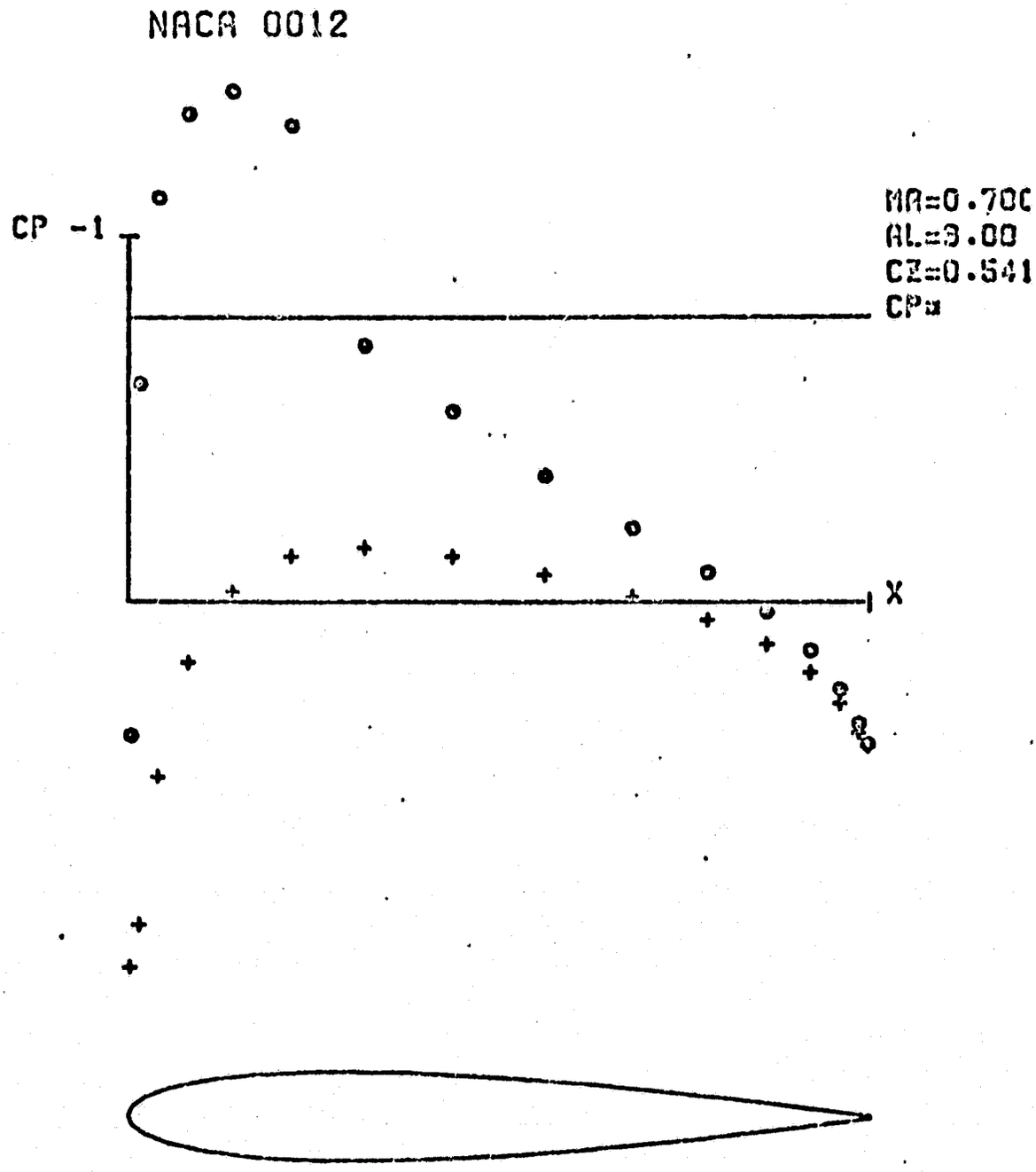


ABB. 12

UFE1352

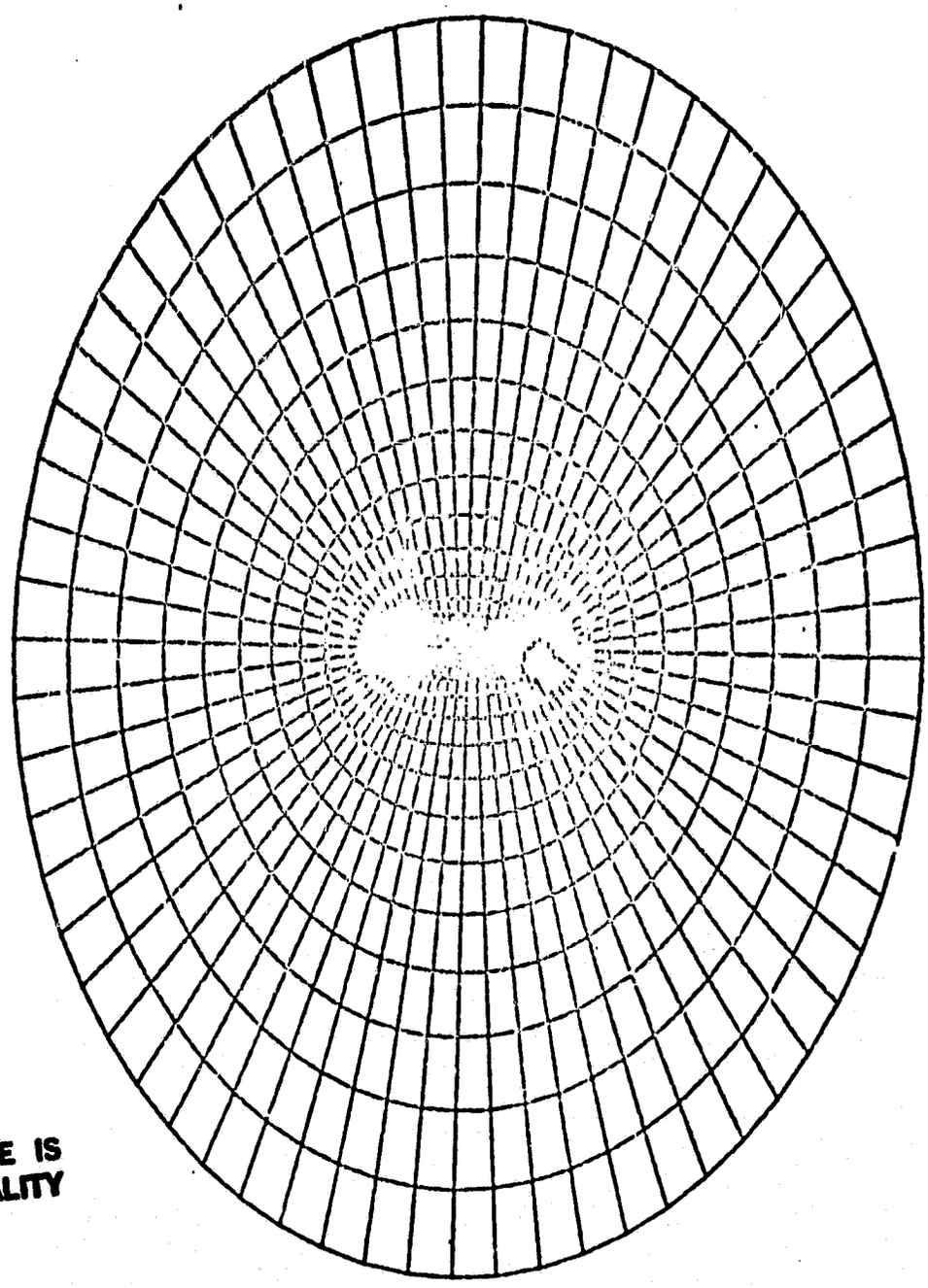



ABB. 13

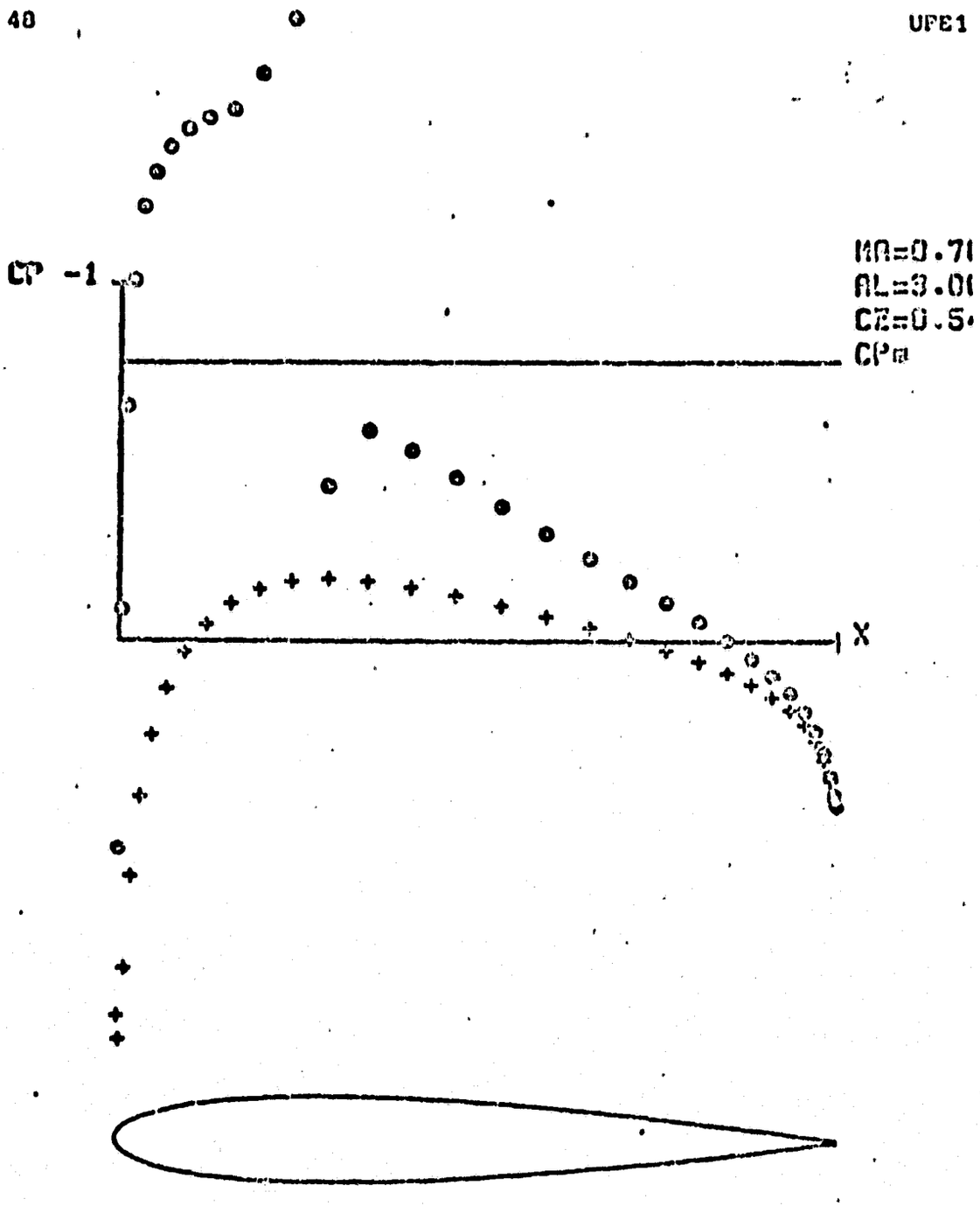


NACA 0012

ADB. 14

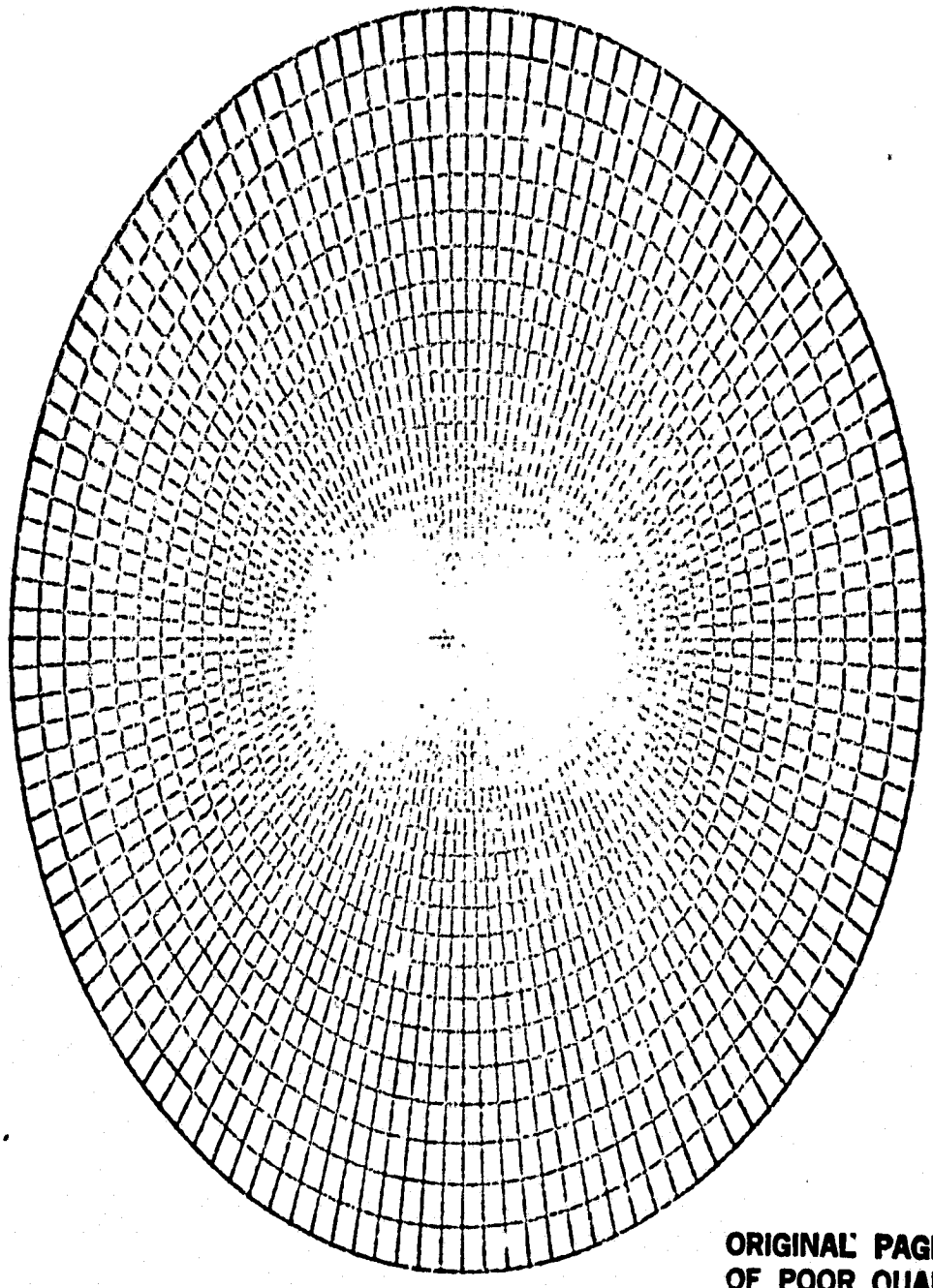



ABB. 15

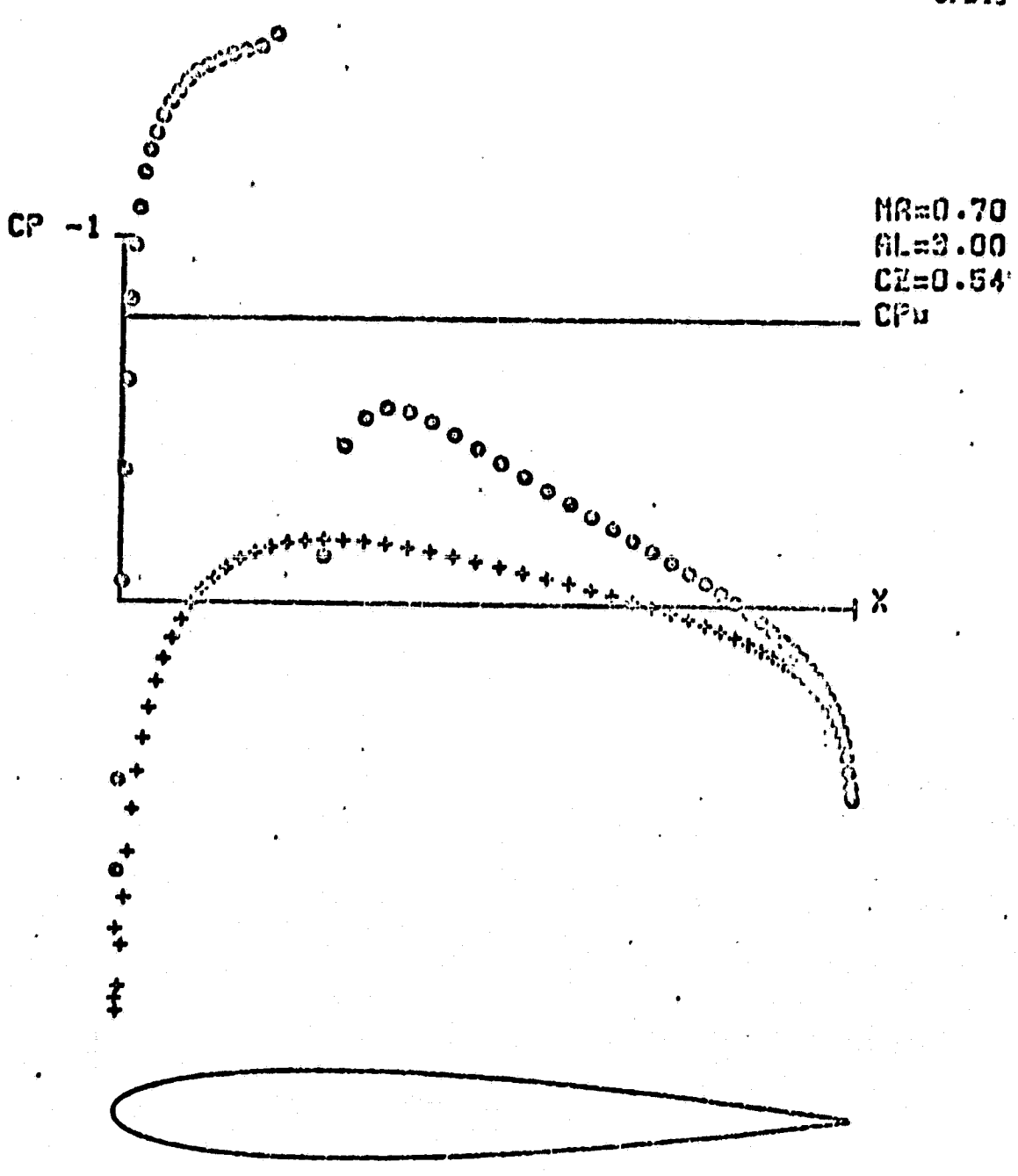


NACA 0012

ABB. 16

UFB1352

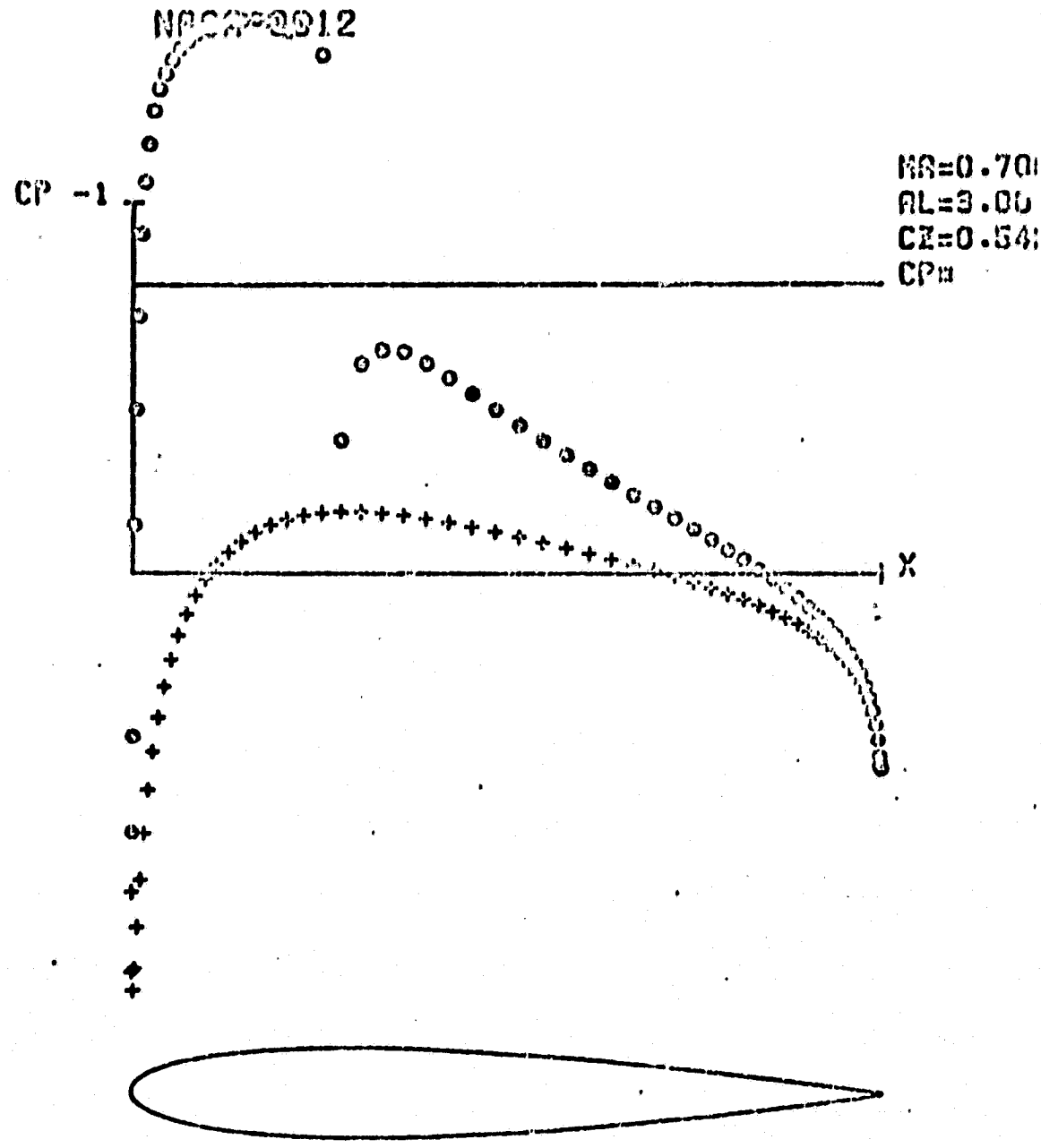


ORIGINAL PAGE IS
OF POOR QUALITY

ABB. 17

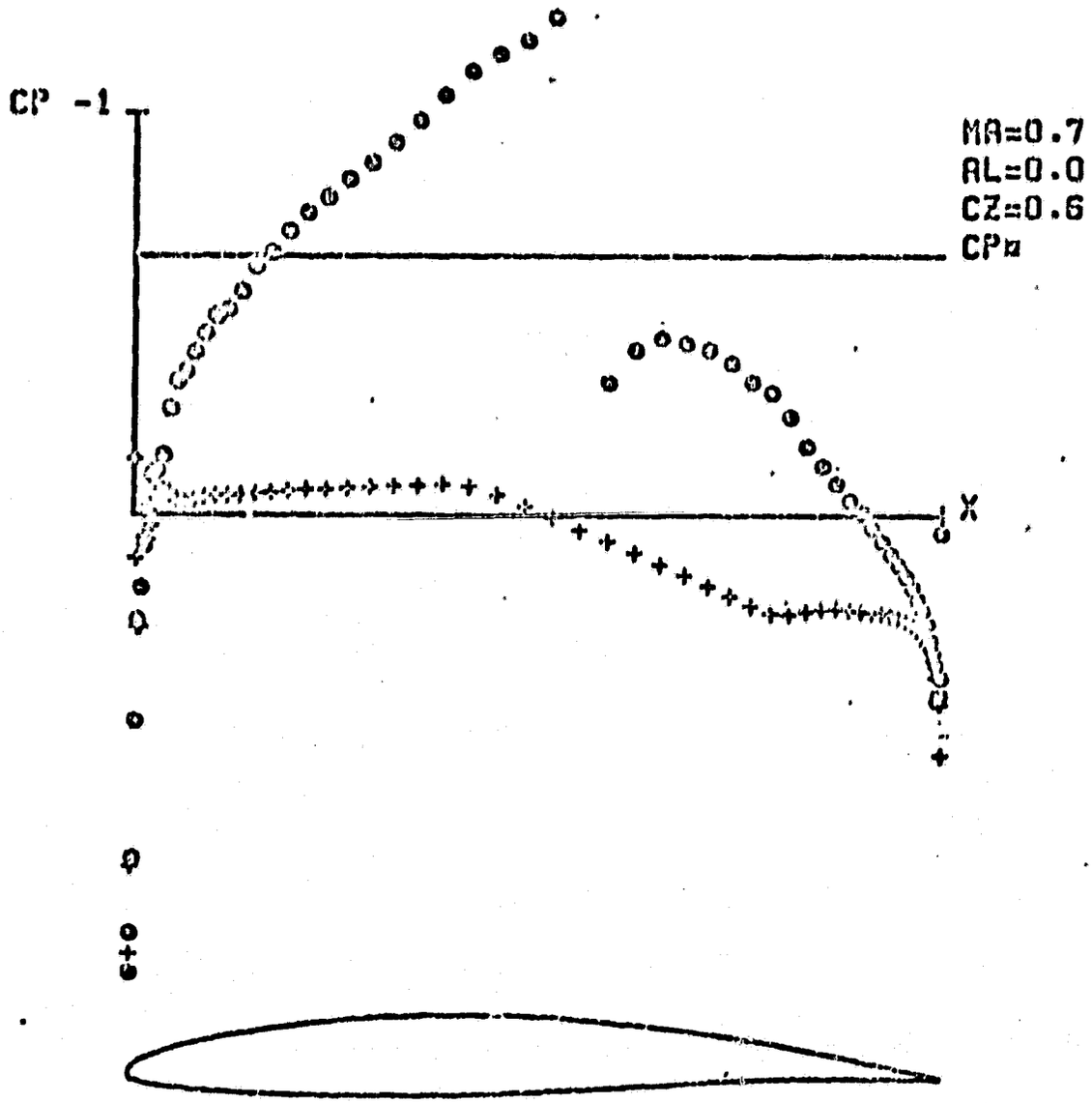


NACA 64A410

ABB. 18

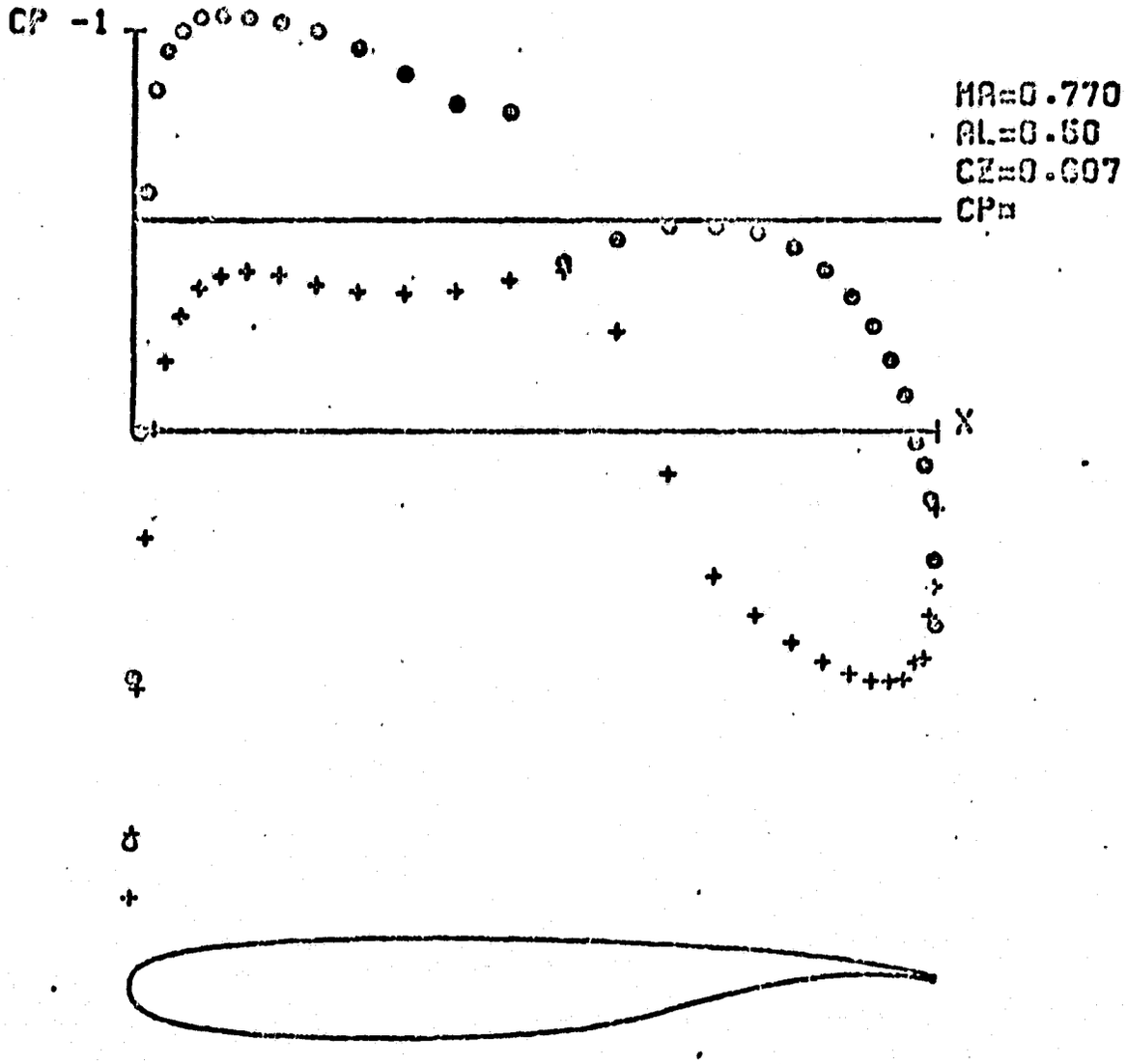


Supercritical profile

UEBERKRITISCHES PROFIL

ABB. 19

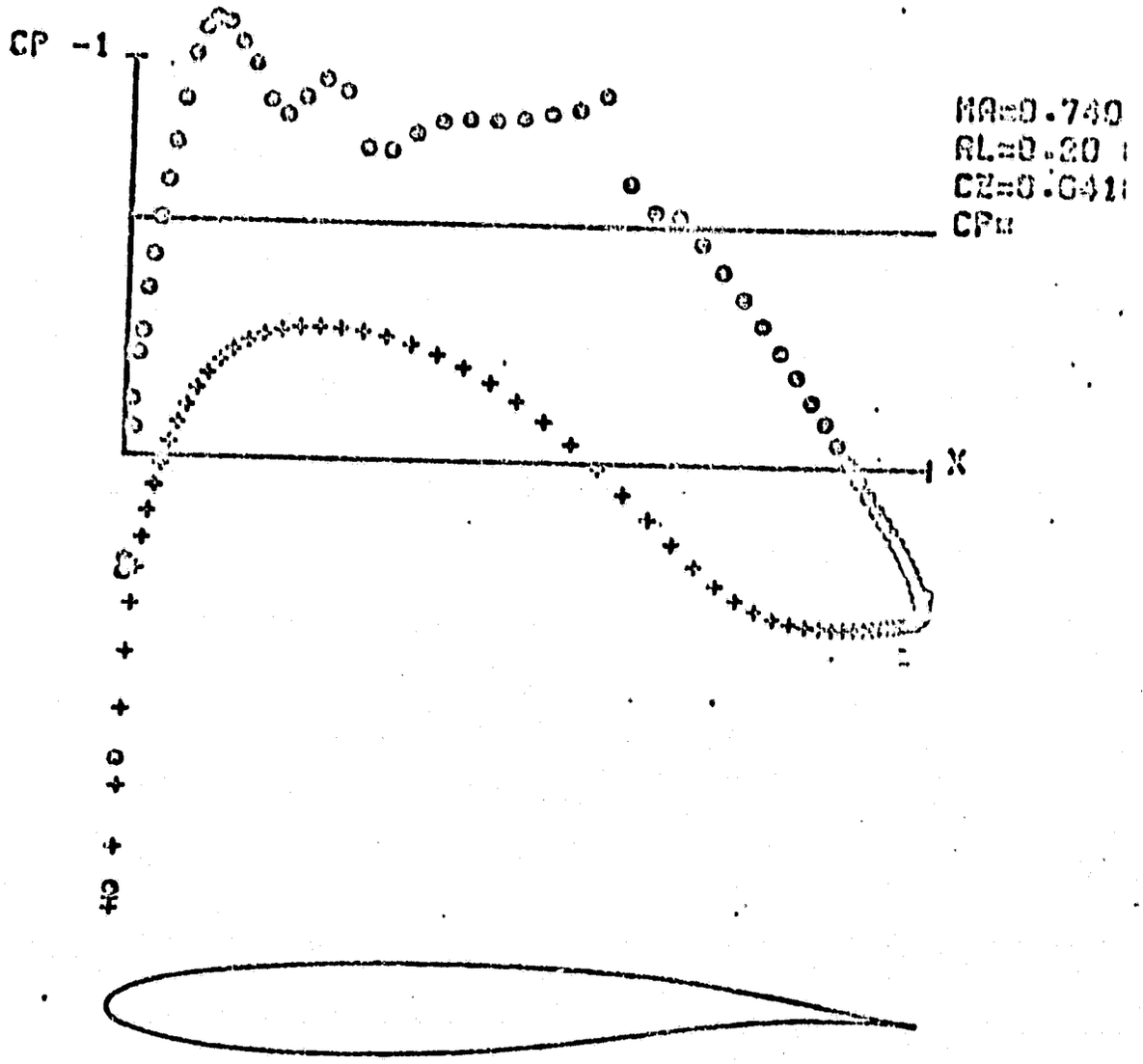


KORN-PROFIL 75-06-12

ABB. 20

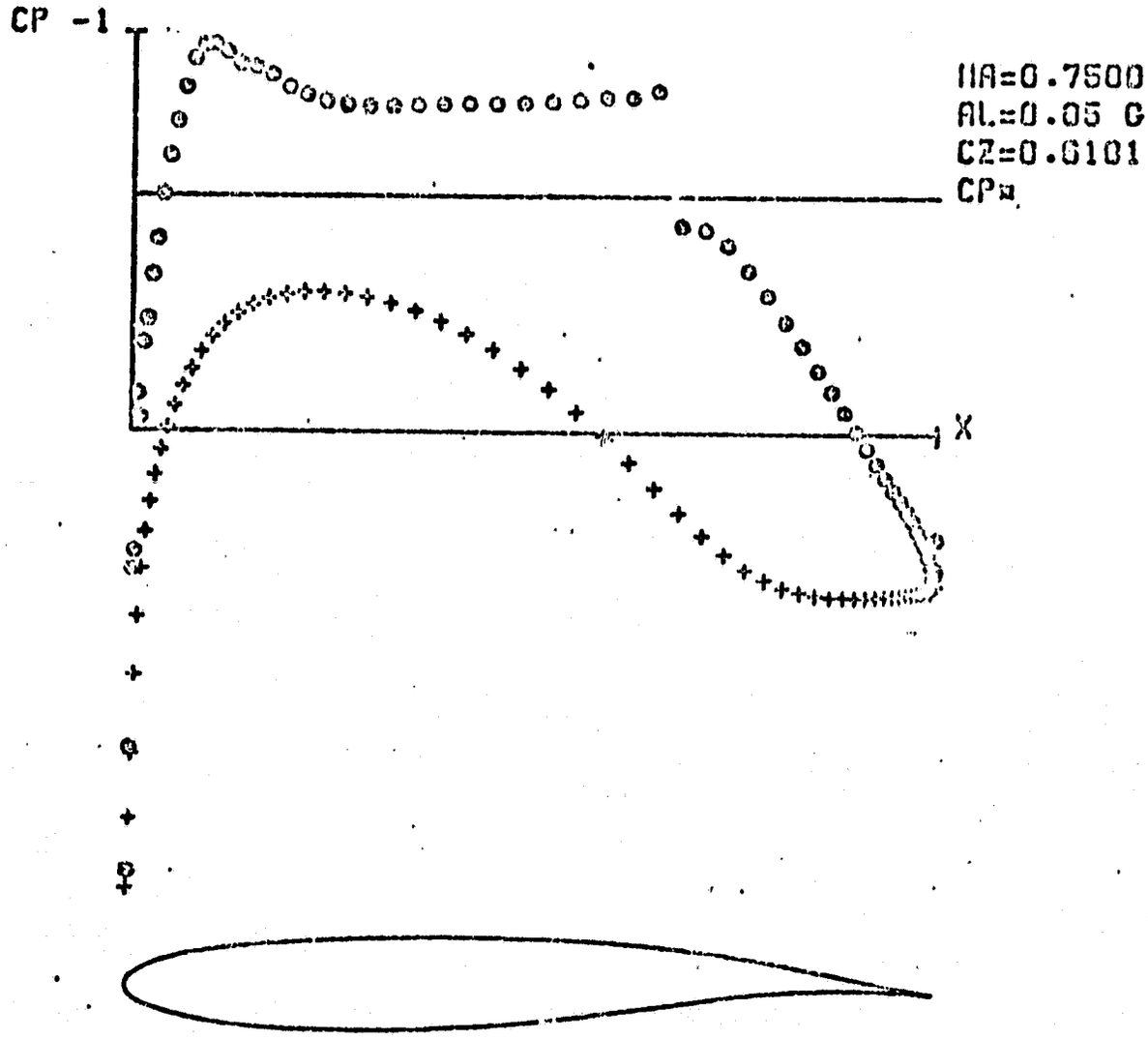




KORN-PROFIL 75-06-12

ABB. 21